Abdominal Radiology (2019) 44:2474–2493
https://doi.org/10.1007/s00261-019-01994-5

REVIEW

The role of multimodal imaging in guiding resectability and cytoreduction in pancreatic neuroendocrine tumors: focus on PET and MRI

Laura Rozenblum[1] · Fatima-Zohra Mokrane[2,3] · Randy Yeh[4] · Mathieu Sinigaglia[5] · Florent Besson[6] · Romain-David Seban[7] · Cecile N Chougnet[8] · Paul Revel-Mouroz[2] · Binsheng Zhao[3] · Philippe Otal[2] · Lawrence H. Schwartz[3] · Laurent Dercle[3,9]

Published online: 12 April 2019

Abstract

Pancreatic neuroendocrine tumors (pNETs) are rare neoplasms that secrete peptides and neuro-amines. pNETs can be sporadic or hereditary, syndromic or non-syndromic with different clinical presentations and prognoses. The role of medical imaging includes locating the tumor, assessing its extent, and evaluating the feasibility of curative surgery or cytoreduction. Pancreatic NETs have very distinctive phenotypes on CT, MRI, and PET. PET have been demonstrated to be very sensitive to detect either well-differentiated pNETs using ^{68}Gallium somatostatin receptor (SSTR) radiotracers, or more aggressive undifferentiated pNETS using ^{18}F-FDG. A comprehensive interpretation of multimodal imaging guides resectability and cytoreduction in pNETs. The imaging phenotype provides information on the differentiation and proliferation of pNETs, as well as the spatial and temporal heterogeneity of tumors with prognostic and therapeutic implications. This review provides a structured approach for standardized reading and reporting of medical imaging studies with a focus on PET and MR techniques. It explains which imaging approach should be used for different subtypes of pNET and what a radiologist should be looking for and reporting when interpreting these studies.

Keywords Neuroendocrine tumors · PET-CT · Theranostics · Somatostatin receptors

Abbreviations

ADC	Apparent diffusion coefficient
AJCC	American Joint Committee on Cancer
APUD	Amine precursor uptake and decarboxylation
CEUS	Contrast-enhanced ultra sound examination
CT	Computed tomography
DOPA	Dihydroxyphenylalanine
DOTATOC	DOTA^0-Phe^1-Tyr^3 octreotide
DWI	Diffusion-weighted imaging
ENETs	European Neuroendocrine Tumor Society
EUS	Endoscopic ultrasound examination

Laura Rozenblum and Fatima-Zohra Mokrane contributed equally to the manuscript.

✉ Laurent Dercle
ld2752@cumc.columbia.edu

[1] Sorbonne Université, Service de Médecine Nucléaire, AP-HP, Hôpital La Pitié-Salpêtrière, 75013 Paris, France

[2] Radiology Department, Toulouse University Hospital, 1 Avenue du Professeur Jean Poulhes, 31059 Toulouse, France

[3] Department of Radiology, New York Presbyterian Hospital, Columbia University, New York, NY, USA

[4] Memorial Sloan Kettering Cancer Center, Molecular Imaging and Therapy Service, New York, NY, USA

[5] Department of Imaging and Nuclear Medicine, Institut Claudius Regaud - Institut Universitaire du Cancer de Toulouse - Oncopole, Toulouse, France

[6] Paris Sud University, Kremlin Bicêtre Hospital, Paris, France

[7] Department of Nuclear Medicine, Institut Curie-René Huguenin, Saint-Cloud, France

[8] Department of Endocrine Oncology, Hôpital Saint Louis, Paris, France

[9] UMR 1015, Gustave Roussy Institute, Université Paris-Saclay, Villejuif 94805, France

^{18}F-FDG	18Fluoro-Fluorodeoxyglucose
^{68}Ga	Gallium-68
^{99m}Tc	Technetium 99m
GLP-1	Glucagon-like peptide 1
IACIG	Intra-arterial injection *of* calcium
IOUS	Intraoperative ultrasound examination
LM	Liver metastases
MEN	Multiple endocrine neoplasia syndrome
MRI	Magnetic resonance imaging
NANETS	North American Neuroendocrine Tumor Society
NF	Neurofibromatosis
NET	Neuroendocrine tumors
OS	Overall survival
PDAC	Pancreatic ductal adenocarcinoma
pNET	Pancreatic tumor
SSTR	Somatostatin receptor
SSTR-PET	Somatostatin receptor PET
SSTR scintigraphy	Somatostatin receptor scintigraphy
SUV	Standard uptake value
TSC	Tuberous sclerosis complex
US	Ultrasound examination
VHL	Von Hippel–Lindau syndrome
WHO	World Health Organization

Introduction

Although pancreatic NETs (pNETs) are relatively uncommon tumors (1 per 100,000 population), they represent 1–2% of all pancreatic neoplasms [1, 2]. Additionally, increasing use of non-invasive diagnostic imaging techniques, as well as increasing availability of imaging techniques worldwide has led to increasing rates of incidental detection of pancreatic NETs, especially non-functional ones [3, 4]. The 5-year overall survival is 85% for G1 and 78% for G2 pNETs [5], explaining their high prevalence compared to other pancreatic neoplasms such as the 8% 5-year survival of pancreatic ductal adenocarcinoma [6]. pNETs have a slight predilection for male (55%) and are typically observed between the third and sixth decades [7]. Earlier presentation of these tumors is generally associated with a familial syndrome. Surgery remains the only curative possibility. Yet, only 20% to 40% of patients diagnosed with pNETs have early-stage curable disease at diagnosis [8].

Medical imaging plays a central role in the diagnosis, staging, and recurrence detection of pNETs, as well as to guide theranostic procedures [9]. Risk stratification is crucial for patients' management: high-risk patients should be guided toward treatment that is more aggressive while therapeutic options should not be exhausted too rapidly in low-risk patients [10, 11]. Predictors of poorer prognosis are Multiple Endocrine Neoplasia Syndrome (MEN), high tumor grade, high tumor burden (e.g., pancreatic insulinomas larger than 2 cm [12, 13]), presence of hormonal syndrome, and non-resectable tumors [14–16]. For resectable tumors, four prognostic factors of metastatic relapse have been validated: tumor size > 5 cm; positive lymph node status; Ki67 proliferative index; and tumor grade [17].

In this article, we review the role of CT, MRI as well as SPECT and PET functional imaging. We report on the real-life experience of how hybrid imaging might lead to improve patient care in pNET and discuss potential future clinical applications and research directions. Additionally, we provide a structured approach for standardized reading and reporting through the proposal of a standardized case report form (Table 1).

Classification of pNETs

Nearly, all well-differentiated pNETs produce hormones and the vast majority are sporadic. The current classification relies on the evaluation of whether production of hormones is sufficient to produce clinical symptoms. Consequently, pNETs are classified as syndromic, non-syndromic, and hereditary.

Tumor imaging phenotype using molecular imaging is strongly associated with tumor grade, which is at the center of patient treatment and management [18]. pNETs are predominantly well-differentiated tumors with endocrine differentiation arising from pluripotent stem cells. The embryological origin of pNETs (foregut) explains that over 80% of NETs overexpress somatostatin receptor (SSTRs) (Figs. 1 and 2). High expression of SSTR on SSTR-specific imaging, and low glucose uptake (on ^{18}F-FDG PET) are indicative of a well-differentiated NETs with low pathological grade, allowing thus to guide patient management [11, 19, 20]. A recent update of WHO Classification for pNETs introduced four categories [21, 22]: Grade 1 well-differentiated NETs (G1 NETs; Ki67 index < 3%; mitotic index < 2/10 high-power microscopic fields); Grade 2 well-differentiated NETs (G2 NETs; Ki67 index 3–20%; mitotic index 2–20/10 HPF); Grade 3 well-differentiated NETs (G3 NETs; Ki67 index > 20%; mitotic index > 20/10 HPF); Grade 3 poorly differentiated neuroendocrine carcinomas (G3 NECs; Ki67 index 3–20%; mitotic index 2–20/10 HPF) [14]. G1-NETs are relatively indolent while G3 NECs have the worst prognosis [14, 15]. Immunohistochemistry differentiates G3 NECs from G3 NETs (Fig. 1).

Syndromic

Functioning NETs are defined by the production of specific hormones, and further characterized by the produced

Table 1 Standardized case report form

Standardized imaging case report form for multidisciplinary tumor board		
Local and regional assessment		
Resectability	Resectable/Non-resectable	
Primary tumor (T)	Location	
	Size	
Local perivascular extension	Y/N	
	Superior than hemicircumferential	Y/N
	Mesenteric extension	Y/N
Local thrombus	Y/N	
	Bland thrombus	Y/N
	Tumor thrombus	Y/N
Local perineural extension	Y/N	
Local lymph node (N)	Involvement	Y/N
	Location	
Metastatic assessment (M)		
Liver	Number of lesion(s)	
	Segment location	I II III IV V VI VII VIII
Lung	Number of lesion(s)	
	Location	URL ML LRL ULL LLL
Axial bone	Number of lesion(s)	
	Location	cervical, dorsal, lumbar spine
	Risk of neurological complication	Y/N
Other bone	Number of lesion(s)	
	Location	
Other metastases	Number of lesion(s)	
	Location	
Imaging phenotype		
SSTR imaging (Krenning score)		1 2 3 4
FDG PET		High/low uptake
DOPA PET		High/low uptake
Treatment eligibility		
Curative surgery		Y/N
Cytoreduction procedures		Y/N
	Surgery	Y/N
		Location
	Thermal ablation	Y/N
		Location
	Surgery/thermal ablation combination	Y/N
		Location
Palliative treatment		Y/N
	Liver embolization	Y/N
		Bland embolization TACE CE-DEB
	SIRT	Y/N
	PRRT	Y/N
	Contraindication for systemic treatment	Y/N

Y/N yes or no, *URL* upper right lung lobe, *ML* middle right lung lobe, *LRL* lower right lung lobe, *ULL* upper left lung lobe, *LLL* upper left lung lobe, *TACE* transcatheter arterial chemoembolization, *CE-DEB* chemoembolization using drug-eluting beads, *SIRT* Selective internal radiotherapy, *PRRT* peptide receptor radionuclide therapy, *FDG* Fluorodeoxyglucose, *DOPA* dihydroxyphenylalanine, *SSTR* somatostatin receptor

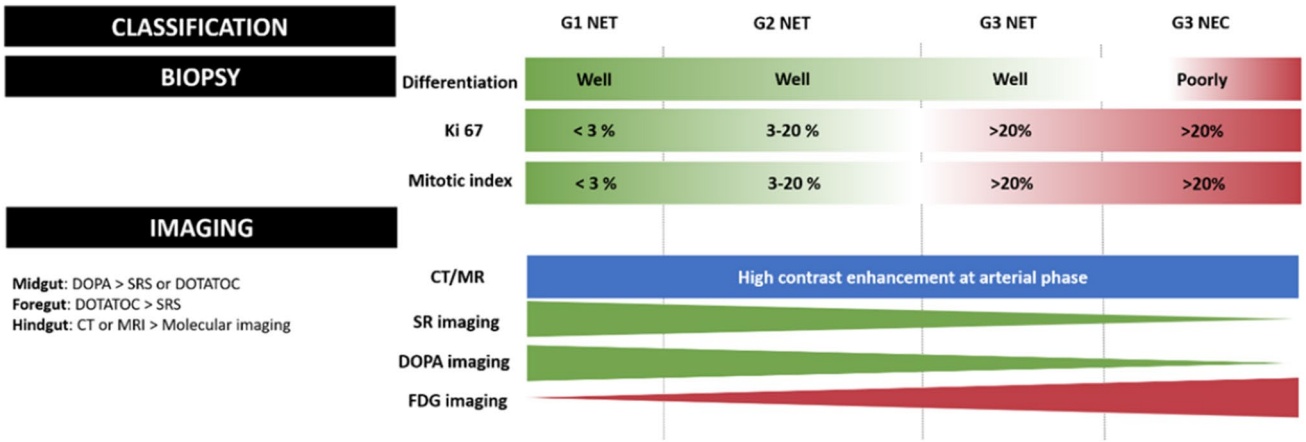

Fig. 1 Imaging phenotype suggests pancreatic NET grade. *G1, G2, G3* Grade 1, 2, or 3. NET: neuroendocrine tumor, *NEC* neuroendocrine carcinoma, *CT* computed tomography, *MRI* magnetic resonance imaging, *FDG* fluorodeoxyglucose, *DOPA* dihydroxyphenylalanine, *DOTATOC* DOTA^{0}-Phe^{1}-Tyr^{3} octreotide, *SRS* somatostatin receptor scintigraphy, *SSTR* somatostatin receptor

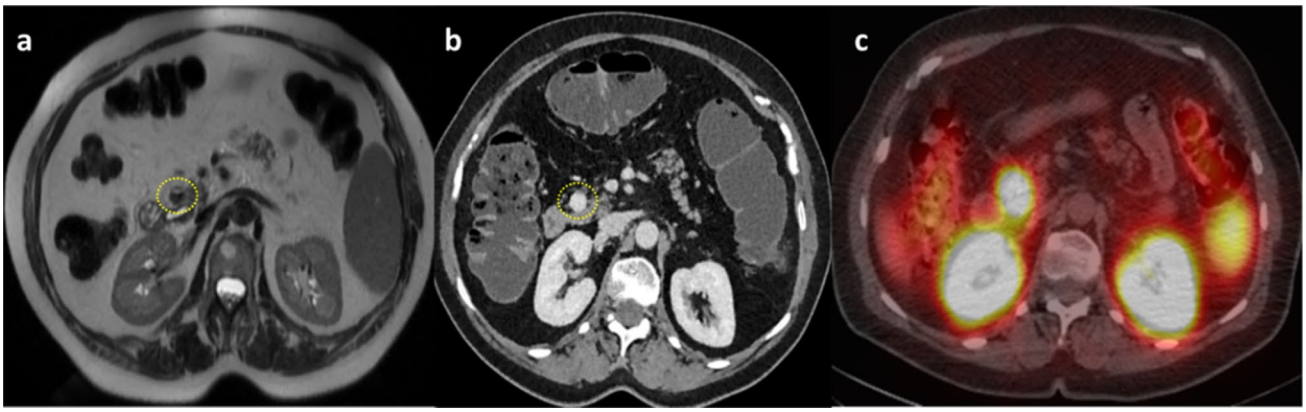

Fig. 2 Well-differentiated syndromic pNET: insulinoma. A 10-mm solitary pancreatic nodule (yellow-dotted circle) located in the pancreas head was assessed using T2-weighted MRI images (**a**), contrast-enhanced CT (**b**) and Somatostatin receptor SPECT/CT performed 24 hours after injection of 111In-pentetreotide (**c**). The lesion appeared with low signal on T2-weighted MRI images (**a**), homogeneously hyper-enhancing on post-contrast CECT (**b**), and high expression of somatostatin receptor which is typically observed in well-differentiated pNETs (**c**). There was no distant metastasis and the primary tumor was considered resectable. After curative surgery, histopathology confirmed the diagnosis of well-differentiated insulinoma

hormones or associated hormonal syndrome. They are observed in up to 40% of pNETs [22, 23]. The prevalence of non-functioning pNETs, which are usually indolent and typically subcentimetric, has increased due to the improvement of imaging capabilities [24–26].

The prognosis of functioning pNETs is driven by clinical symptoms (i.e., hypoglycemias in functioning insulinomas). However, the functional status should be considered for the choice of the imaging protocol. For instance, the identification of dehydration or dysglycemia could preclude the acquisition of contrast-enhanced CT and 18F-FDG PET [23, 29, 30]. Additionally, imaging may fail to visualize small tumor foci of functioning NETs detected biochemically [20].

The main types of functioning pNETs are insulinoma (50% of functioning pNETS) followed by gastrinoma, glucagonoma, and VIPomas. The majority of insulinoma are benign, solitary, intrapancreatic lesion smaller than 2 cm in size. A typical presentation is the Whipple triad with fasting hypoglycemia, symptoms of hypoglycemia, and relief of symptoms after the intra venous administration of glucose. Gastrinoma is the second most frequent. They are often small (1–3 cm) and multiple, and the majority is malignant, intra-pancreatic, and in the gastrinoma triangle which is localized between cystic duct/common duct insertion, pancreatic neck, and junction of 2nd/3rd portions of the duodenum (Fig. 3). The typical presentation is Zollinger–Ellison Syndrome characterized by large amount

of gastrin secretion, leading to peptic ulcers and diarrhea. Glucagonoma and VIPomas are usually large at diagnosis with distal topography within the pancreas and frequently malignant [24–26].

Non-syndromic

Non-functioning NETs are typically detected later due to non-specific symptoms such as pain and mass effect [27]. They have an unpredictable behavior and risk to metastasize [28]. Although non-functioning pNETs tend to be larger and more heterogeneous at diagnosis than functioning pNETs [29], medical imaging is not used to predict functional status. When compared to syndromic tumors, non-syndromic tumors are typically larger at presentation, more likely to be malignant (80–100%), to have a heterogeneous appearance (cystic, calcification, necrosis) and to be aggressive [24–26] (Figs. 4 and 5).

Hereditary

Although the majority of NETs occurs sporadically (up to 85%) [30], an hereditary syndrome, such as Multiple Endocrine Neoplasia Syndrome (MEN)1, Von Hippel–Lindau (VHL), neurofibromatosis I (NF), and tuberous sclerosis complex (TSC) should always be ruled out [30, 31]. MEN type 1 is highly associated with gastrinoma (50%) but also VIPomas, Glucagonomas, somatostatinomas, GRHomas, ACTHomas, and PTHrp-omas. These rare functioning pNETs are usually malignant, metastatic at diagnosis [3, 18, 32, 33], and can be functioning (carcinoids syndrome or hypercalcemia) (Fig. 5) [27, 34].

VHL pancreatic involvements include cysts (40%), serous cystadenoma (10%), and pNET (15%), which are frequently solitary, non-syndromic presentation and are malignant in 8 to 50%. Other abdominal manifestations are renal cysts, clear cell renal cell carcinoma, and pheochromocytoma. On MRI, a background of multiple diffuse cystic replacement can be observed.

NF is responsible for skin, central, and peripheral nervous system tumors, as well as neurodegenerative and musculoskeletal abnormalities. pNETs occur in up to 10% of patients with NF1. TSC can cause tumor of several organs such as the skin, brain, lung, heart, and gastrointestinal system. pNETs are also relatively uncommon in TSC with a prevalence of 2 to 9% [35].

Diagnosis and detection: CT, MR, and EUS

First-line imaging techniques are CT, MRI (e.g., diffusion-weighted imaging sequences), and endoscopic ultrasound for local assessment (Tables 2 and 3) [32]. Despite the small size of pNETs, sensitivity of CT (30 to 80%) and MRI (85%) are high [36]. Typical appearance of pNETs is a small, well-defined solitary, and uniform mass of 1-5cm of diameter [35]. Contrast-enhanced CT and MRI are standard of care imaging for pNETs [37] as they appear typically hypervascular during the late arterial enhancement phase [32, 37–39]. Moreover, the DWI related Apparent Diffusion Coefficient (ADC) could be correlated to tumor grade as

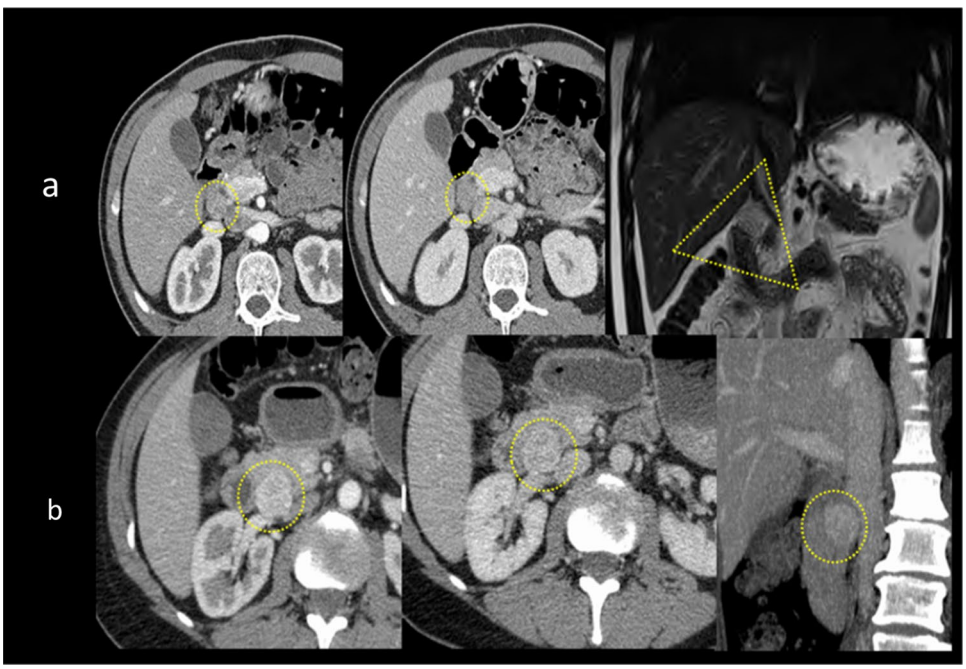

Fig. 3 Frequent locations of pNETs: anatomical imaging. **a** Gastrinoma are typically located in the "gastrinomas triangle" (yellow dotted triangle). Extra-pancreatic nodule measuring 10 mm located in the gastrinomas triangle with homogeneous arterial (right), and portal contrast enhancement (middle). **b** Insulinoma are more often localized in the pancreas head. This case shows a 25-mm nodule with arterial (right), and portal contrast hyperenhancement (middle). The report should always include the absence of vascular and perineural involvements (as well as distal metastases) in order to confirm the resectability

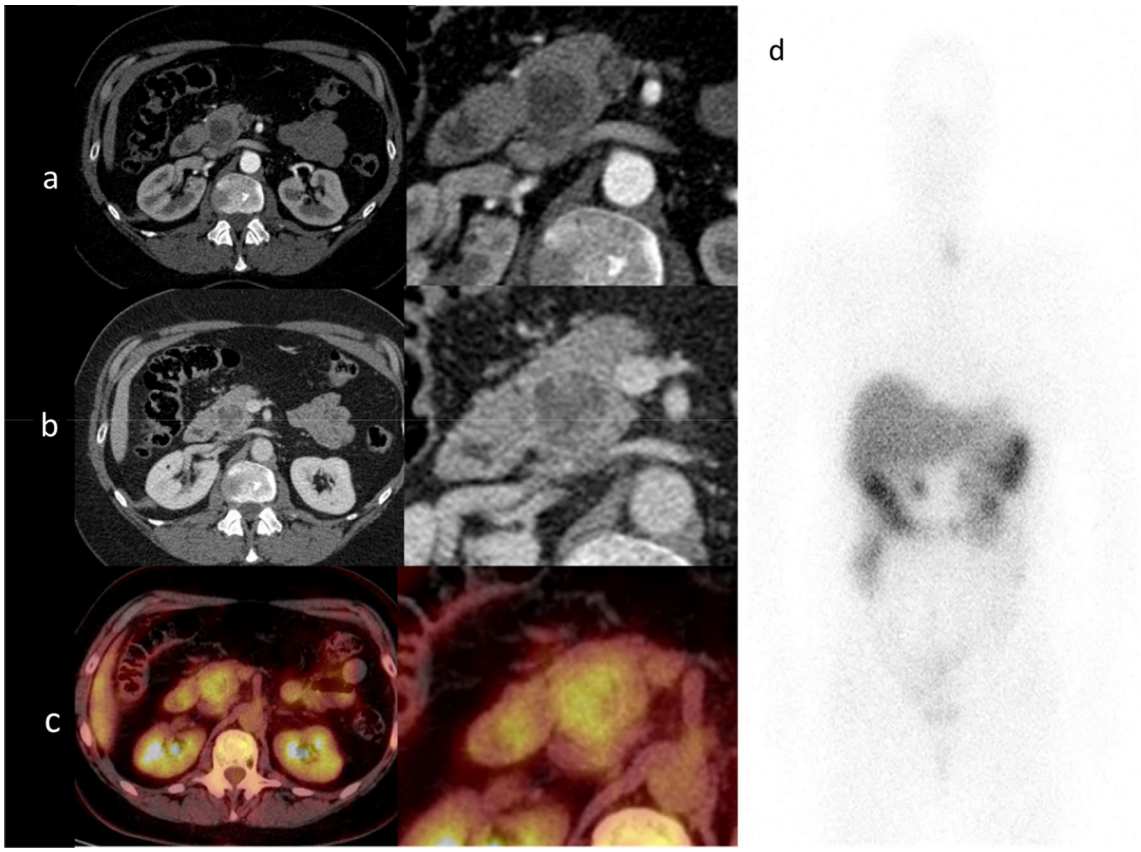

Fig. 4 Non-syndromic pancreatic NET. Incidental detection of a non-syndromic 15-mm pancreatic lesion with low arterial contrast enhancement (a), low heterogeneous portal enhancement (2), low ^{18}F-FDG uptake (2), and intermediate SSTR expression (d). Imaging phenotype suggested a well-differentiated resectable pNET, later confirmed by curative surgery

tumor cellularity in higher tumor grade causes restriction of motion of water molecules, and ADC cutoff values of less than 0.95×10^{-3} to 1.19 mm^2/s have been proposed for G3 tumors [24–26].

Endoscopic ultrasound (EUS) has a high sensitivity (80 to 90%) especially for patients with negative CT examinations: up to 10% of insulinomas are not detected [3], and 40% are smaller than 1 cm [12, 13, 32]. It allows excellent locoregional characterization of biliopancreatic ductal involvement, and local biopsy procedures. EUS is however rather invasive, operator dependent, and has lower sensitivity for distal pancreatic area [24–26, 40].

Tumor appearance: hyperenhancement pattern

Most of functioning PNETs are well-defined small tumors with intense and homogeneous enhancement on arterial and portal phases (Fig. 2). This enhancement phenotype is the most specific one regarding NETs [36]. However, a more fibrous content may be observed and responsible for a more delayed enhancement on the delayed phase. On MRI, they appear with low signal on T1-weighted sequence, intermediate to high signal on T2-weighted sequence, hyper-enhancing on post-contrast, and diffusion restricting (Fig. 6). The enhancement pattern is varied and can be homogenous, heterogeneous, or ring-like, especially in gastrinomas [24–26] (Figs. 2, 4, 5, 6). Differential diagnosis include pancreatic ductal adenocarcinoma, intrapancreatic accessory spleen, and hypervascular metastases to the pancreas (most often related to renal cell carcinoma) [24–26].

Moreover, up to 50% of pNETs may not show arterial hyperenhancement and many still demonstrate iso- to hyperenhancement on venous phase. Hypoenhanced (on arterial and venous) pNETs are more likely to be higher grade and more difficult to differentiate from pancreatic adenocarcinoma (Fig. 4) [24–26].

In insulinoma, the isoenhancement can make them difficult to identify on CT, whereas the soft tissue contrast properties of MRI (T1 hypointensity, mild T2 hyper intensity, and diffusion restriction compared to the physiological pancreatic background) can help to detect the lesion on MRI.

In gastrinomas, MR images are T1 hypointense on precontrast phase, and T2 hyperintense, and diffusion-restricting

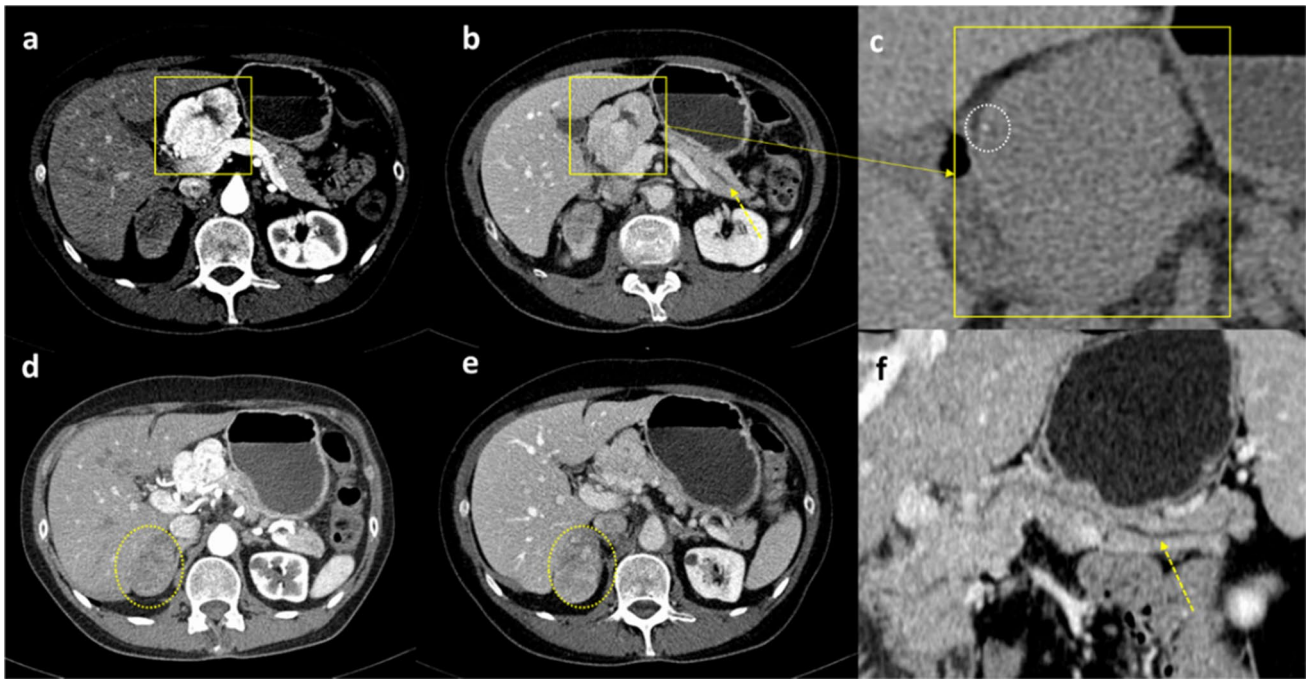

Fig. 5 Multiple endocrine neoplasia syndrome. Pancreatic NET (**a**, **b**, **c**) associated with pheochromocytoma (**d**, **e**). Pancreatic NET appears as a heterogeneous hypervascular mass (yellow box, **a** and **b**), with a dot-shaped microcalcification (white dotted circle). Curved coronal reconstruction of the portal CT examination reveals the absence of ductal dilation (**f**, yellow-dotted arrow). In type 1 MEN syndrome, pNETs can be associated with pituitary adenoma and/or pheochromocytomas. In this case, abdominal CT reveals a heterogeneous right adrenal mass (**d** and **e**). Before the surgery, the patient was appropriately prepared with medications such as alpha-blockers that blocked the effects of adrenaline

Table 2 Indications of medical imaging in PNETS

Anatomic imaging	Molecular imaging
Pancreatic NET (all)	
CT[a] and/or MRI[b]	^{68}Ga-DOTATOC-PET or SSTR scintigraphy ^{18}F-DOPA-PET
Insulinoma	
IACIG (if difficult to localize)	^{18}F-DOPA-PET GLP-1 receptor scintigraphy (if difficult to localize)
Gastrinoma	
IACIG (if difficult to localize)	^{68}Ga-DOTATOC-PET GLP-1 receptor scintigraphy (if difficult to localize)
Poorly differentiated	
CT[a] and/or MRI[b]	^{18}F-FDG PET

IACIG selective intra-arterial injection of calcium with hepatic venous insulin gradients, *DOPA* dihydroxyphenylalanine, *DOTATOC* DOTA^{0}-Phe^{1}-Tyr^{3} octreotide, *SSTR* scintigraphy: somatostatin receptor scintigraphy

[a]Reconstruction < 3 mm. Contrast-enhancement (acquisition: 15-25s after injection for angiography phase, 25-30s for portal-venous inflow phase, 70-90s for venous phase)

[b]Fat-saturated transaxial T1- weighted and fat-saturated T2-weighted sequences and optionally fat-saturated transaxial in and out of phase T1-weighted sequences. Transaxial dynamic gadolinium contrast-enhanced sequences with acquisition at 30, 70, and 120 s and at 3–5 min after the injection. Diffusion-weighted imaging

DWI and T2FS. After contrast injection, gastrinomas have often a persistently delayed enhancement due to the presence of fibrosis [40]. Additionally, a marked gastric wall thickening can be observed.

Table 3 Summary of the role of the most common imaging techniques used in pNETs

CT	MRI	US	Somatostatin SPECT/PET	^{18}F-DOPA PET	^{18}F-FDG PET
Main indication					
All pNETs, for local and distant evaluation	Pancreatic MRI: disease localization Assessment of liver metastases	Livers metastases: assessment, biopsy, thermal ablation	Foregut NETs	Insulinomas in children	Undifferentiated
Technical points					
High spatial resolution Multiplanar imaging High sensitivity for small bowel lesions	Spatial resolution less good than CT Absence of radiation	Absence of radiation exposure	No need of an on-site cyclotron to synthetize ^{68}Ga-DOTATOC Higher sensitivity of ^{68}Ga-DOTATOC-PET vs SSTR scintigraphy	High specificity	Easily available Lower cost
Clinical points					
Initial assessment, localization, staging, restaging, and definition of margins for operability High sensitivity for pulmonary and hepatic lesions Availability, rapidity, and reproducibility Biopsy guidance for thoracic lesions	Localization, staging, restaging, definition of margins for operability High sensitivity for pancreatic and hepatic lesions -Visualization of biliary and pancreatic ducts (CP-MRI) Use of organ-specific contrast media	Transabdominal US or *CEUS*: possible characterization of dubious lesions at CT/MRI *EUS* high sensitivity for pancreatic NETs, guidance for biopsy *IOUS* delineation for liver and pancreatic lesions before resection	Diagnosis and staging of grade 1 and 2 NETs of any embryological origin Follow-up of grade 1 and 2 NETs of any embryological origin Patient selection for PRRT	Staging and detection of recurrence of well-differentiated NETs of the digestive tract Detection of unknown primary lesion of G1 or G2 NETs when SSTR scintigraphy/PET is negative or unavailable. Diagnosis and localization of insulinomas in the case of hyperinsulinism in infants and children	Localization of NECs and high-grade poorly differentiated NETs (Ki67≥20%)
False negatives					
Small lesions. Non-respect of NET-dedicated scanning protocols (e.g., no arterial or no portal venous phases)	Non-respect of NET-dedicated protocols (e.g., no arterial or portal venous phase, no diffusion-weighted images)	*Trans abdominal US* non- or less echoic patients *EUS* pancreatic NETs located at pancreatic tail	Small lesions High background activity like liver, kidney, and spleen is difficult		Differentiated NETs
False positives					
Other benign/malignant lesions especially if underlying liver disease	Diffusion-weighted images present a high sensitivity, with less high specificity	Other benign/malignant lesions especially if underlying liver disease	Physiological uptakes: pancreatic uncinate process, accessory spleen, or intrapancreatic spleen Meningioma, neural crest tumors, or clear cell renal carcinoma	Physiological uptake of biliary ducts or ureters	Inflammation, infection

Table 3 (continued)

CT	MRI	US	Somatostatin SPECT/PET	^{18}F-DOPA PET	^{18}F-FDG PET
Theranostics					
Biopsy or thermal ablation procedures guidance for liver/abdominal lesions therapies (RFA, MW…)	Biopsy or thermal ablation procedures guidance for oligo metastatic hepatic or pulmonary locations lesions (not common)	*Trans abdominal US* biopsy or thermal ablation procedures guidance for liver/abdominal lesions *EUS* guidance for biopsy *IOUS* biopsy or thermal ablation procedures guidance during surgery (enucleation)	177Lu or 90Y–DOTA-peptides		Resection of undifferentiated ^{18}F-FDG+ tumors

US ultrasound examination, *CEUS* contrast-enhanced ultra sound examination, *EUS* endoscopic ultra-sound examination, *IOUS* intraoperative ultrasound examination, *CT* computed tomography *MRI* magnetic resonance imaging, *^{18}F-FDG* 18Fluoro-Fluorodeoxyglucose

Duct dilation

Duct dilation is associated with higher grade of pNETS, although such appearance may be easily confused with a pancreatic ductal adenocarcinoma (PDAC). The degree of dilation and related atrophy is typically less than that of PDAC. Vascular invasion is also uncommon (Figs. 5 and 6).

Cystic pNET

Cystic is an uncommon appearance that occurs in 10 to 20% of pNETs and cystic lesions may have better prognosis than solid lesions [1, 41–43]. Most cystic PNETs present larger in size than solid PNETs and are commonly non-functioning [24–26, 40]. Pancreatic NETs may be partially or entirely cystic. Hyper-enhancing thickened wall, especially during arterial phase is characteristic. This appearance may overlap with some other cystic neoplasms of pancreas. On MRI, a centrally T2 bright cystic lesion can be identified with typically a thick rim of enhancement. The differential diagnosis is a necrotic adenocarcinoma with heterogeneous (vs. homogeneous) T2 signal and irregular (vs. smooth) peripheral and central (vs. peripheral) enhancement. Another differential diagnosis is mucinous cystic neoplasm which typically occurs in female in the sixth decade, appearing as large unilocular cyst with thickened enhanced wall (Fig. 7).

Calcifications

Calcifications are uncommon and occurs in 10–20% of pNETs. They are associated with larger, higher-grade tumor and are more likely to be metastatic. The calcifications are typically coarse, focal, and irregular but can also be dot-shaped (Fig. 5). These calcifications may be observed in the primary tumor as well as the metastases. Calcifications in NET are predominantly observed in a solid and hyperenhancing lesion with focal, coarse, irregular central calcifications. Several studies described the differential diagnoses of a calcified pancreas mass.[44–47] In predominantly cystic lesions, calcification can occur in a pseudocyst (outer rim calcification), mucinous cystic neoplasm (curvilinear or punctate calcification), serous cystic neoplasm (central calcified scar), and intraductal papillary mucinous neoplasm (intraductal calcification). In predominantly solid and hyperenhancing lesions, calcifications can occur in adenocarcinoma (calcification adjacent to the mass) and focal pancreatitis (focal calcifications). In solid tumors with variable enhancement and variable calcifications patterns, the diagnoses are acinar cell carcinoma, calcified metastasis, and pancreatoblastoma. There are several differential diagnoses of calcifications in the pancreatic parenchyma such as chronic pancreatitis, calculus (intraductal), vascular lesions (involving arterial wall

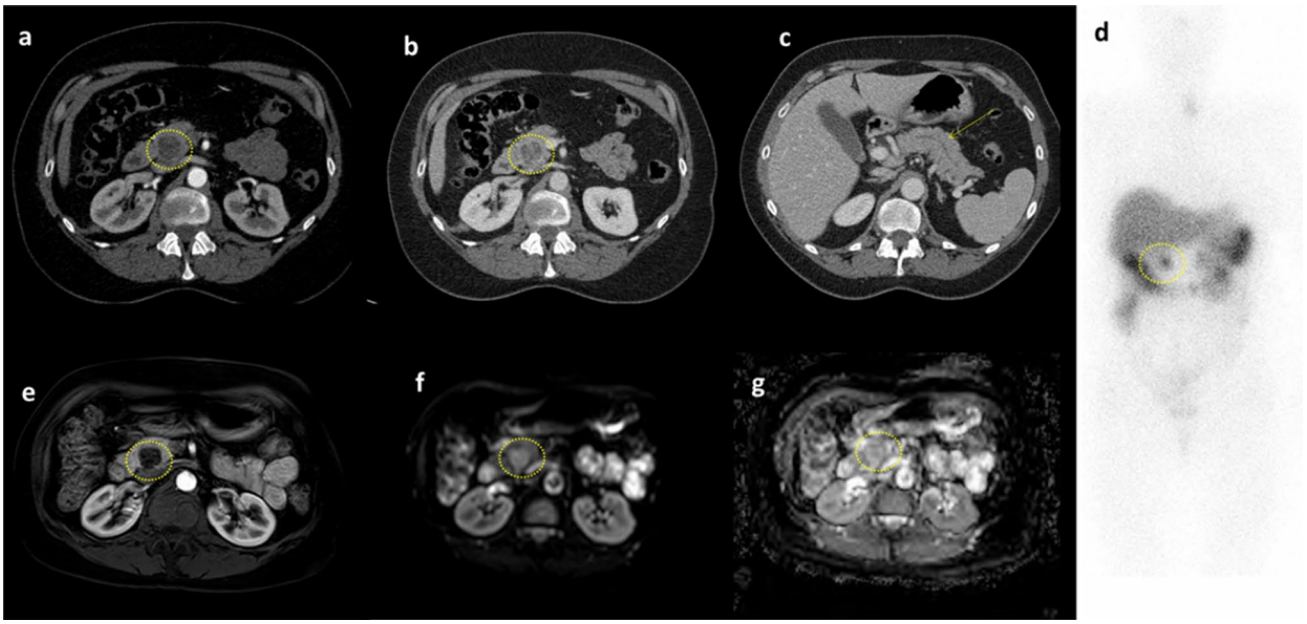

Fig. 6 Atypical phenotype: Hypovascular non-syndromic pNET. International consensus guidelines recommend routine surgical resection, ranging from tumor enucleation to pancreatectomy (+/− duodenectomy) with lymphadenectomy in all non-metastatic non-syndromic pNETS larger than 2 cm. This 17-mm non-syndromic pNET (yellow-dotted circles) appears hypodense on arterial CT (**a**), heterogeneous and still hypodense on portal phase (**b**), with no Wirsung duct dilation (**c**, yellow arrow). Somatostatin Receptor Scintigraphy suggests a well-differentiated pNET due to the high somatostatin receptor expression (**d**). An active follow-up has been performed in this patient for 6 years using MRI to decrease radiation exposure. Six years later, the lesion remains stable and measures 17 mm (**e**, **f** and **g**). On MRI, the lesion is hypovascular on arterial contrast-enhanced images (**e**), showing hypersignal on B=800 diffusion images (**f**), and no ADC restriction (**g**)

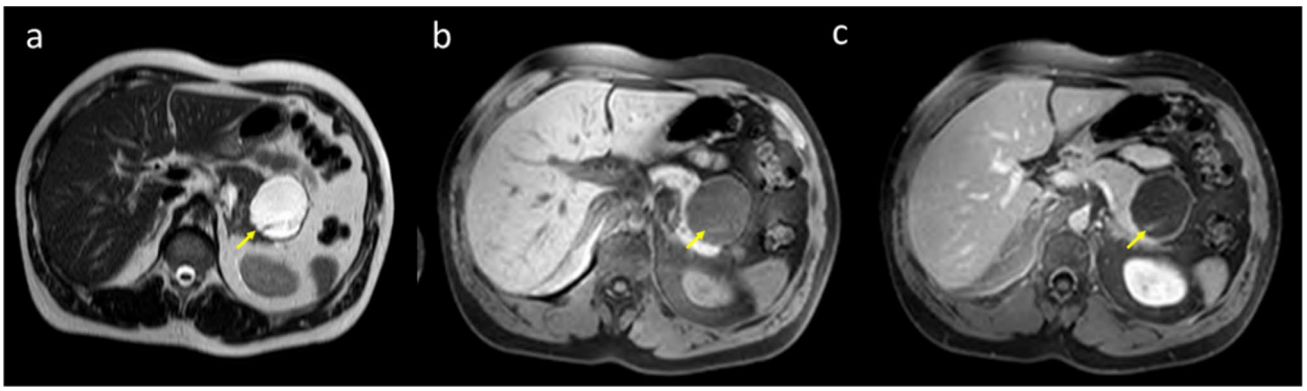

Fig. 7 Non-syndromic cystic pNET. Incidental detection of a cystic pancreatic NET. Assessment using T2-weighted sequence (**a**), T1 FATSAT-weighted sequence (**b**), and T1 FATSAT after gadolinium injection (**c**). There is a 3-cm thin-walled cystic lesion in the pancreas tail (**a**, **b**, **c**) without mural hyperenhancement (**c**). The unique posterior septation (yellow arrows) appears as a linear iso-intensity on T2-weighted sequence (**a**), hypointensity on T1 FATSAT-weighted sequence (**b**), and enhanced after gadolinium injection (**c**). International consensus guidelines recommend routine surgical resection in all non-metastatic non-syndromic pNETS larger than 2 cm. After curative surgery, pathology showed a cystic pNET

or aneurysm), infectious cysts due to tuberculosis, sarcoidosis, parasitic infestations (isolated pancreatic hydatid and pancreatic cysticercus) as well as rare diagnosis such as pancreatic schwannoma (von Recklinghausen disease), epidermoid cyst in an intrapancreatic accessory spleen (Stippled calcification), a mature cystic teratoma (calcification and fat), and gene-associated pancreatitis [44–47].

Diffuse growth pattern

Rare cases showing a diffuse growth pattern with replacement/enlargement of a large segment or the entire pancreas are described in literature. This pattern is associated with higher-grade tumors and poorer prognosis [48].

Diagnosis and detection: molecular imaging

Somatostatin receptor imaging

Up to 80% of NETs overexpress SSTR. Therefore, SSTR imaging is indicated for the diagnosis, staging, and follow-up of G1 and G2 pNETs. Six different SSTRs have been identified: SSTR1, 2A, 2B, 3, 4, and 5 [49] but NETs mainly overexpress SSTR2 and SSTR5 [50].

SSTR2 scintigraphy using 111Indium-pentetreotide (Octreoscan) was standard-of-care in this setting during many years [11, 51]. However, SSTR PET using gallium-68 (68Ga)-radiolabeled SSTR is now the preferred imaging method [11], due to several technical advantages: shorter study length, higher spatial resolution and sensitivity detection (^{68}Ga-DOTATOC PET: 90–95%, SSTR scintigraphy: 60–80%) [19, 20]), tracer uptake quantification, and significant radiation reduction [52, 53]. Also radiochemistry of ^{68}Ga is advantageous as (i) the ^{68}Ga radio-isotope is produced by generator; (ii) this trivalent metal can be easily linked to somatostatin analogs using chelators (DOTATATE, DOTATOC, and DOTANOC, for example); (iii) It can then be easily replaced by therapeutic radio-isotope linked to the same vector (^{90}Yttrium or ^{177}Lutetium, for example) to perform theranostics [47, 54]. DOTATATE shows 10-fold higher and selected affinity for SST-2 receptor, DOTATOC high affinity for SST-2 even if less than DOTATATE, and also for SST5 receptor and DOTANOC high affinity for SST-2 SST-3 and SST5 subtype receptors [40]. Studies have demonstrated no clinical impact of those different chelators, and no preferential use of one compound over the others can be advised [55]. False positives include physiological uptake in the pancreatic uncinate process, accessory spleen, or intra-pancreatic spleen. The differential diagnosis includes other primary tumor types overexpressing SSTR, such as neural crest tumors or clear cell renal carcinomas [30]. False negatives are observed in small lesions and organs with high physiological background activity such as the liver, kidney, and spleen [31, 32] (Tables 2 and 3).

SSTR antagonists PET were recently explored by several studies. Antagonists targeted essentially SSTR2 and used 3 chelators: DOTA, NODAGA (1,4,7-triazacyclononane, 1-glutaric acid-4,7-acetic acid, and CB-TE2A (4,11-bis (carboxymethyl)-1,4,8,11-tetraazabicyclo [6.6.2] hexadecane). On preclinical studies, they were labeled either with ^{64}Cu or ^{68}Ga. Preliminary results have shown favorable pharmacokinetics, high tumor-to-background contrast, and better sites labeling than agonists [56].

Amino-acid imaging: ^{18}F-DOPA-PET

^{18}F-DOPA is a cost-effective and increasingly available technique. ^{18}F-DOPA PET reflects the amino acids metabolism by exploiting the amine precursor uptake and decarboxylation property of neuroendocrine cells. In pNETs, ^{18}F-DOPA-PET is currently the gold standard for the diagnosis and localization of insulinomas (i.e., hyperinsulinemia of infants and children) [11], which remains challenging for CT, MRI, and EUS. Nakuz et al. have demonstrated a sensitivity of 70% of combined ^{18}F-DOPA PET with contrast-enhanced CT. Usefulness of carbidopa premedication, an inhibitor of the peripheral aromatic amino acid decarboxylase is still debated as it can cause a masking effect on tumor uptake [57]. In the case of physiological high background activity (pancreas), early PET acquisition may be of interest [11].

Glucose imaging: ^{18}F-FDG-PET

In poorly differentiated NETs, PET imaging takes high advantage of the increased glycolytic rates related to the Warburg effect [58, 59] of proliferative cells such as cancer cells. Cancer cells use aerobic glycolysis for their metabolism instead of the oxidative phosphorylation pathway used by most other cells. As a glucose analogue, ^{18}F-FDG is transported into cells via glucose transporters, phosphorylated by hexokinase, but does not undergo the rest of glycolysis, allowing accumulation within cells. ^{18}F-FDG PET is recommended for G3 NETs and NECs with Ki-67 > 20% [11]. ^{18}F-FDG detects 92% of NETs with Ki-67 > 15% [60] (Fig. 2). Prospective studies demonstrated that ^{18}F-FDG positivity in G1/G2 NET is not rare (13% of patients) and is a strong predictor of poorer prognosis and higher risk of progression [61]. Recently, Bucau et al have shown that some well-differentiated tumors with a proliferation index of less than 2% might show ^{18}F-FDG uptake (SUVmax of > 2), potentially due to sporadic VHL gene inactivation. [62] However, glucose intolerance is a frequent complication of pancreatic tumors. Elevated serum glucose levels can decrease the ^{18}F-FDG uptake in the pancreatic tumor and is responsible for most false-negative results on ^{18}F-FDG-PET [63].

Management of biochemically positive and imaging negative patients

First-line imaging procedures may be negative and fail to visualize small tumor foci of functioning NETs detected

biochemically [32]. In these cases, second-line imaging procedures should be used.

Glp-1 receptor scintigraphy

Insulinomas overexpress GLP-1 receptors on their surface [64, 65]. Scintigraphy with a radiolabeled Glucagon-like peptide 1 (GLP-1) receptor analog may be useful in functioning insulinomas with negative anatomical imaging. Several radiotracers were tested in this indication. However, ^{99m}Tc radiotracer seems to outperform others in detecting GLP-1 receptors due to its high sensitivity, low price, its accessibility, and its low radiation rates [65, 66]. While sensitivity of this technique is ranging from 95 to 100%, its lacks of specificity is up to 25% [67]. Therefore, use of GLP-1 imaging is limited to insulinomas that are not detected using other imaging techniques. This technique is not standard of care and limited to few expert centers. Additionally, it still requires validation in large series [3, 65].

Intra-arterial injection of calcium with hepatic venous insulin gradients (IACIG)

IACIG and GLP-1 receptor scintigraphy are the two major highly sensitive methods used to localize occult insulinomas. IACIG is a highly sensitive technique which detects the expression of calcium-sensing receptors (expressed in insulinomas and gastrinomas) [3, 68–71]. This interventional diagnostic approach uses the vascular pancreatic segmentation to selectively determine insulin secretion source. After selective arterial injection of calcium gluconate, insulin secretion is measured by hepatic venous catheterization at different time points, and thus determine insulinomas location. For instance, high insulinemia after selective injection of the gastroduodenal artery suggests an insulinoma in the head of the pancreas. IACIG shows a sensitivity up to 93% in segmental localization of insulinomas [72].

Rationale for PET/MRI

A PET/MRI protocol offers the possibility of a one-stop-shop examination, which can streamline workflow and patient quality of care (Fig. 8) [73]. Integrated PET/MRI has a potential edge over PET/CT since the attenuation

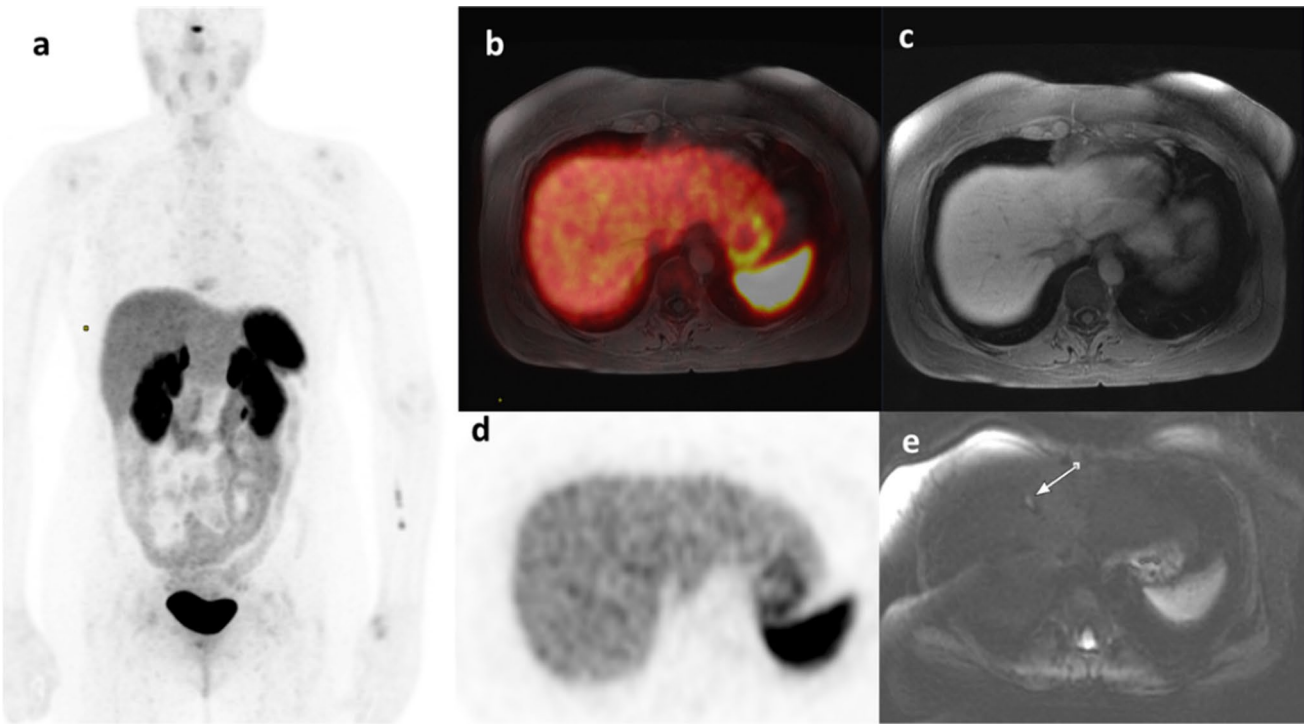

Fig. 8 Active follow-up after curative surgery using PET/MRI. A well-differentiated grade 2 pNET was surgically removed. A ^{68}Ga-DOTATATE PET/MR was performed because of an increasing of neuroendocrine tumor transcripts. On DOTATATE PET no abnormal uptake was detected, (**a** MIP), especially on the liver (**b**, **d**). There was no enhancing lesion on post-contrast sequence (**c** post-contrast MR and **d** PET fusion with post-contrast MR. Only diffusion-weighted images (**b** 500) sequence revealed a small focus of restricted diffusion in segment IVA/VIII, suspicious of liver metastasis (**e**, white arrow). This case demonstrates the superiority of MR over other imaging modalities for liver assessment

correction CT component of standard PET/CT is usually a free-breathing dataset that is acquired at a very low radiation dose and without intravenous contrast [73]. Additionally, simultaneous acquisition of PET and MRI data and advanced motion correction algorithms [74] result in better temporal and spatial co-registration although they require a significant expertise and are used systematically in all PET/MR devices. This is a significant advantage allowing for decreasing mis-registration artifacts and motion artifacts between PET and CT due to their sequential acquisition [73]. This advantage might be leveraged to increase the performance of PET for the detection of lesions in the primary tumor site, as well as the locoregional extent in the retroperitoneal compartment [75–78].

Combining relevant MRI sequences to PET acquisitions may potentialize the strengths of the two modalities, especially for abdominal imaging [79–81]. The high soft-tissue contrast of MRI combined to the high sensitivity of PET detection makes this procedure a challenging candidate for pNETs imaging. Moreover, PET/MRI multiparametric combinations may improve the tumor characterization, by increasing the level of imaging features deciphering the tumor-imaging phenotype [82]. Minimizing radiation exposure of patients by substituting CT-scan by MRI must be put into perspective in patients with potentially curable resectable pNET, with long overall survival rates.

There is, however, one downside for the use of PET/MRI [83]. CT-scan clearly outperforms MRI for attenuation correction, which is the key role of morphological imaging although several new MR-based approaches have been shown to substantially improve the PET-MRI images quality [84–86]. The attenuation correction based on MRI data is indeed satisfactory for basic diagnostic purpose, but does not reach the performance of the CT-based attenuation correction, because of the non-continuous properties of the MRI-based generated mu-maps [87–90]. An option is to use T1-Water 3D Dixon and T1-Fat 3D Dixon sequences prior to contrast administration which allows a segmentation of the attenuation map into 4 automatically generated classes (i.e., background, lungs, fat, and soft tissue) which can alter the measurement of SUV [91, 92] since attenuation correction is continuous on CT-scan while it is discrete on MRI. Such consideration may be of relevance especially for quantitative purpose. This should be taken into account for radiomics approaches deciphering intratumor heterogeneity which require to carefully monitor acquisition protocols [93–98]. This needs also to be considered when PET is performed to optimize dosimetry planning but should theoretically not significantly alter the evaluation of the resectability of pNET when a qualitative or semi-quantitative approach is sufficient.

The co-registration of MRI and PET/CT (lower time of acquisition, better cost-effectiveness, and more accurate attenuation correction) might be more convenient for several centers than PET/MRI. The benefits of those procedures for patients' outcome, clinicians, and the healthcare system remain to be determined. The main advantage is that it will minimize the bias in term of co-registration and allows for a multiparametric approach and to integrate functional MR and molecular imaging at a voxel-wise level of analysis.

Patient management

Accurate staging of pNETs is essential to determine proper patient management, particularly in identifying patients who will benefit from surgical resection [3]. Preoperative staging has a dual objective: on one hand to determine the resectability of the primary tumor and on the other hand to evaluate for distant metastasis that would preclude curative resection. Resectable pNETs patients have an excellent prognosis with 75% disease-specific survival at 20 years [99].

Locoregional staging

Vascular invasion may be present in up to one-third of large non-syndromic tumors and is important to search for in all patients since it alters the resectability of the tumor. The splenic vein is more commonly involved than the superior mesenteric vein or artery, and smaller branch veins. Local perivascular and perineural evaluation is critical for staging and guiding surgery [100, 101]. For instance, in pNET, report should include the location of vascular and perineural involvements and its extent since it typically precludes resectability [100, 102] (Fig. 9).

General staging

Surgical resection is considered as the definitive curative treatment by all international guidelines [103]. However, locoregional and distant involvement must be excluded before surgery, because of high rates of post-operative complications. Both pNETS TNM staging system and AJCC cancer staging agree that presence of lymph node metastases is a poor prognostic factor regarding tumor recurrence after surgery [3]. MRI detection of lymph node metastasis has shown acceptable results but is outperformed by ^{68}Ga-DOTATOC-PET/CT [39, 104].

The risk of distant metastatic spread is proportional to the size of the primary tumor (< 1 cm: 20% compared to > 2 cm: 70%) [18]. Common sites of distant metastases include the liver, which are associated with a poorer prognosis, and present with intense arterial enhancement similar to the primary pancreatic tumor [30, 105–107]. The detection of metastases is crucial prior to surgery with curative intent. However, the presence of metastases does not preclude

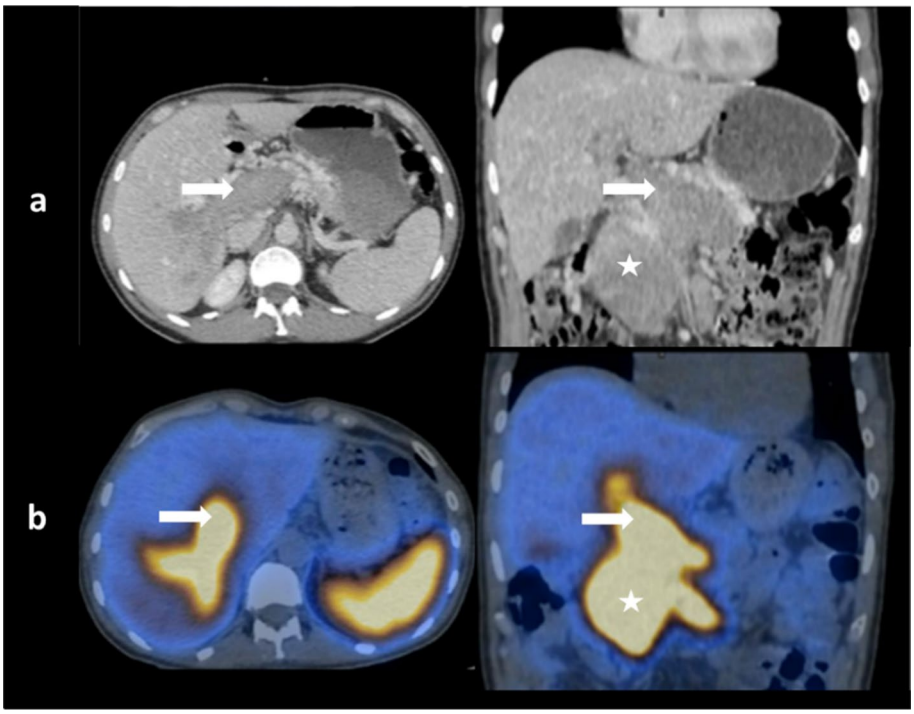

Fig. 9 Tumor thrombus precluding surgical resectability. Well-differentiated pNET (grade 2) with vascular extension to the portal vein, superior mesenteric vein, and the splenomesenteric trunk. The tumor (**a**, white stars) as well as the thrombus inside the portal vein and its branches (white plain arrows) show contrast enhancement at the portal venous phase. SRS (**b**) show high SSTR expression in both tumor (white star) and thrombus (white dotted star). The differential diagnoses were a bland thrombus and a tumor thrombus. The presence of contrast enhancement and of somatostatin receptor expression within the thrombus confirmed a tumor thrombus precluding tumor resectability

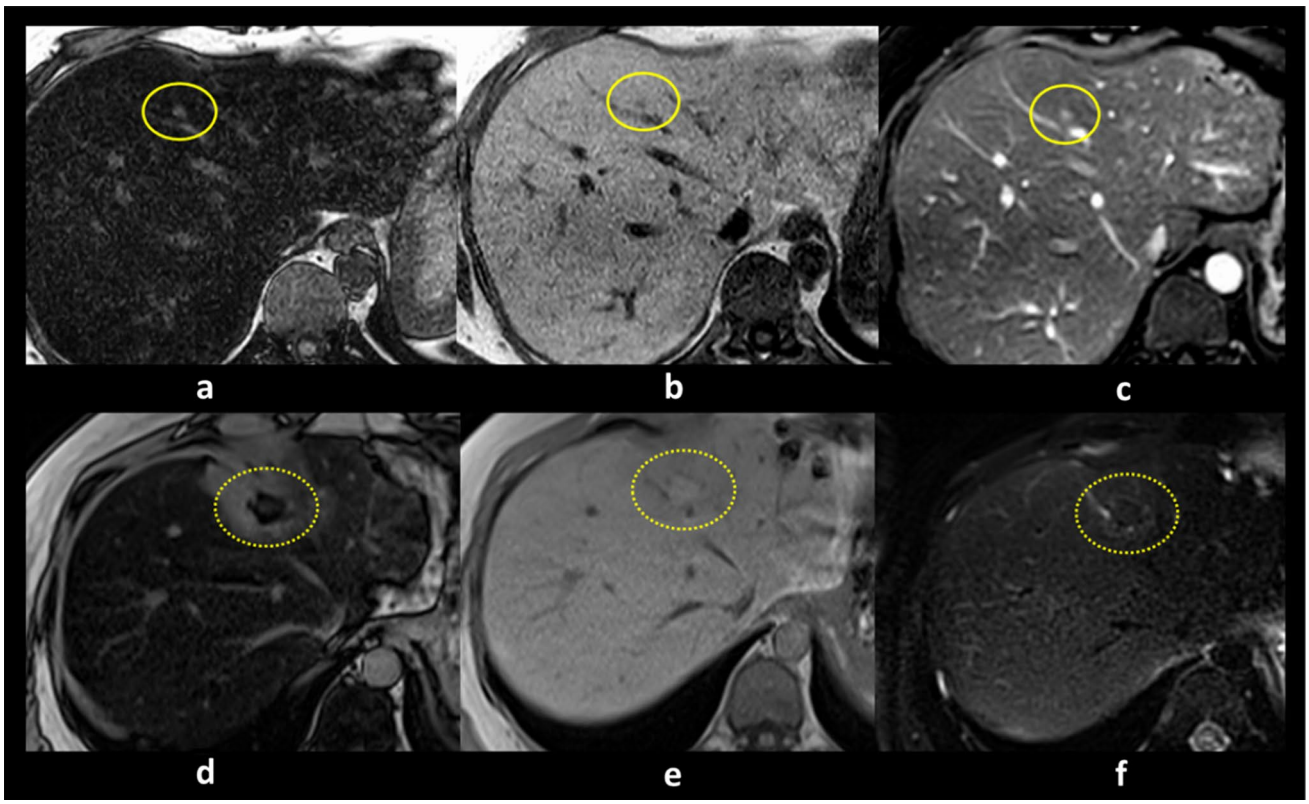

Fig. 10 Detection and treatment of liver metastases: concept of cytoreduction. Initial staging (**a**, **b** and **c**) of a locally resectable pNET showed a unique small liver metastasis (yellow circles), identified using out of phase (**a**), barely identified on T1-weighted images (**b**) but presenting arterial contrast enhancement (**c**). A cytoreduction approach was decided and the metastasis was treated using US-guided radiofrequency ablation. MR imaging after cytoreduction (**d**, **e** and **f**) confirmed that ablation margins were acceptable (yellow-dotted circles) and the treatment was successful

cytoreduction to decrease hormonal symptoms, improve quality of life, and increase survival. The detection rate of metastases varies among techniques. For instance, ^{68}Ga-DOTATOC-PET/CT outperforms MRI for the detection of pulmonary lesions, whereas MRI is superior for liver and bone lesions [104, 108].

Surgery

International consensus guidelines recommend routine surgical resection, ranging from tumor enucleation to pancreatectomy (+/− duodenectomy) with lymphadenectomy; in all non-metastatic non-functioning, GEP-NETS larger than 2 cm, as this strategy results in a significant survival benefit [3]. The optimal management of non-functioning GEP-NETS smaller than 2 cm is still debated, although a non-operative approach with active follow-up is recommended [3, 18, 28]. Surgical resection, is also proposed in curative intent to all patients with operable well-differentiated metastases from NET regardless of the site of origin (foregut, midgut, hindgut) [109].

Cytoreduction

Palliative debulking is beneficial only for patients with liver metastases or abdominal lymph nodes [110] and usually only performed when more than 90% of tumor burden can be removed [111]. The exact assessment of number and location of liver metastases is crucial for treatment planning, and will be mainly based on MRI imaging [112, 113]. Local liver treatment with thermal ablation is indicated in patients with small oligometastatic disease and is as effective as surgery with fewer complications [113–115]. Intra-arterial interventional radiology procedures techniques are reserved for symptomatic patients with hepatic-predominant, non-resectable NETs [18, 116]. Pretreatment imaging will help patients' assessment and reduce rates of incomplete treatments (or inadequate therapy).

Thermal ablation procedures are frequently used in liver metastases and can be combined with surgery, for palliative debulking or curative intent. Radiofrequency ablation is the only proven procedure according to international guidelines, yet, alternative methods (cryotherapy, microwave coagulation) might also be as effective, but need evaluation with randomized control trials (Fig. 10) [111, 117].

Conclusion

Multimodality imaging is critical in the proper management of patients with pNETs. The role of hybrid functional imaging with PET/CT and PET/MRI in pNETs continues to evolve as our understanding of these modalities expands. Imaging-guided approaches help to personalize patient management and will continue to improve quality of life and survival for pNETs patients. Imaging can provide a comprehensive non-invasive evaluation of the spatial and temporal heterogeneity of the tumor, as well as a broad spectrum of information such as stage, grade, resectability, behavior, growth potential, sensitivity to treatment of the primary, and metastatic disease (Fig. 6). This review provides a standardized case report form on Tables 1 and 2.

Funding L Dercle's work was funded by a grant from Fondation Philanthropia, Geneva, Switzerland, and the Fondation Nuovo-Soldati.

Compliance with ethical standards

Conflict of interest All authors declare no conflict of interest.

Ethical approval This article does not contain any studies with human participants or animals performed by any of the authors.

References

1. Canellas R, Lo G, Bhowmik S, Ferrone C, Sahani D (2018) Pancreatic neuroendocrine tumor: Correlations between MRI features, tumor biology, and clinical outcome after surgery. J Magn Reson Imaging 47 (2):425-432. https://doi.org/10.1002/jmri.25756
2. Smith JK, Ng SC, Hill JS, Simons JP, Arous EJ, Shah SA, Tseng JF, McDade TP (2010) Complications after pancreatectomy for neuroendocrine tumors: a national study. J Surg Res 163 (1):63-68. https://doi.org/10.1016/j.jss.2010.04.017
3. Falconi M, Eriksson B, Kaltsas G, Bartsch DK, Capdevila J, Caplin M, Kos-Kudla B, Kwekkeboom D, Rindi G, Klöppel G, Reed N, Kianmanesh R, Jensen RT, Participants aoVCC (2016) ENETS Consensus Guidelines Update for the Management of Patients with Functional Pancreatic Neuroendocrine Tumors and Non-Functional Pancreatic Neuroendocrine Tumors. Neuroendocrinology 103 (2):153-171. https://doi.org/10.1159/000443171
4. Vagefi PA, Razo O, Deshpande V, McGrath DJ, Lauwers GY, Thayer SP, Warshaw AL, Fernández-del Castillo C (2007) Evolving patterns in the detection and outcomes of pancreatic neuroendocrine neoplasms: the Massachusetts General Hospital experience from 1977 to 2005. Archives of Surgery 142 (4):347-354
5. Ellison TA, Wolfgang CL, Shi C, Cameron JL, Murakami P, Mun LJ, Singhi AD, Cornish TC, Olino K, Meriden Z, Choti M, Diaz LA, Pawlik TM, Schulick RD, Hruban RH, Edil BH (2014) A single institution's 26-year experience with nonfunctional pancreatic neuroendocrine tumors: a validation of current staging systems and a new prognostic nomogram. Ann Surg 259 (2):204-212. https://doi.org/10.1097/sla.0b013e31828f3174
6. Siegel RL, Miller KD, Jemal A (2017) Cancer Statistics, 2017. CA Cancer J Clin 67 (1):7-30. https://doi.org/10.3322/caac.21387
7. Halfdanarson TR, Rabe KG, Rubin J, Petersen GM (2008) Pancreatic neuroendocrine tumors (PNETs): incidence, prognosis and recent trend toward improved survival. Ann Oncol 19 (10):1727-1733. https://doi.org/10.1093/annonc/mdn351

8. Ambe CM, Nguyen P, Centeno BA, Choi J, Strosberg J, Kvols L, Hodul P, Hoffe S, Malafa MP (2017) Multimodality Management of "Borderline Resectable" Pancreatic Neuroendocrine Tumors: Report of a Single-Institution Experience. Cancer Control 24 (5):1073274817729076. https://doi.org/10.1177/1073274817729076
9. van Essen M, Sundin A, Krenning EP, Kwekkeboom DJ (2014) Neuroendocrine tumours: the role of imaging for diagnosis and therapy. Nat Rev Endocrinol 10 (2):102-114. https://doi.org/10.1038/nrendo.2013.246
10. Halfdanarson TR, Rabe KG, Rubin J, Petersen GM (2008) Pancreatic neuroendocrine tumors (PNETs): incidence, prognosis and recent trend toward improved survival. Annals of Oncology 19 (10):1727-1733. https://doi.org/10.1093/annonc/mdn351
11. Bozkurt MF, Virgolini I, Balogova S, Beheshti M, Rubello D, Decristoforo C, Ambrosini V, Kjaer A, Delgado-Bolton R, Kunikowska J, Oyen WJG, Chiti A, Giammarile F, Fanti S (2017) Guideline for PET/CT imaging of neuroendocrine neoplasms with (68)Ga-DOTA-conjugated somatostatin receptor targeting peptides and (18)F-DOPA. Eur J Nucl Med Mol Imaging 44 (9):1588-1601. https://doi.org/10.1007/s00259-017-3728-y
12. Gouya H, Vignaux O, Augui J, Dousset B, Palazzo L, Louvel A, Chaussade S, Legmann P (2003) CT, Endoscopic Sonography, and a Combined Protocol for Preoperative Evaluation of Pancreatic Insulinomas. American Journal of Roentgenology 181 (4):987-992. https://doi.org/10.2214/ajr.181.4.1810987
13. Berends FJ, Cuesta MA, Kazemier G, van Eijck CH, de Herder WW, van Muiswinkel JM, Bruining HA, Bonjer HJ (2000) Laparoscopic detection and resection of insulinomas. Surgery 128 (3):386-391. https://doi.org/10.1067/msy.2000.107413
14. Klöppel G, Klimstra DS, Hruban RH, Adsay V, Capella C, Couvelard A, Komminoth P, La Rosa S, Ohike N, Osamura RY, Perren A, Scoazec J-Y, Rindi G (2017) Pancreatic Neuroendocrine Tumors: Update on the New World Health Organization Classification. AJSP: Reviews & Reports 22 (5)
15. Tang LH, Basturk O, Sue JJ, Klimstra DS (2016) A Practical Approach to the Classification of WHO Grade 3 (G3) Well Differentiated Neuroendocrine Tumor (WD-NET) and Poorly Differentiated Neuroendocrine Carcinoma (PD-NEC) of the Pancreas. The American journal of surgical pathology 40 (9):1192-1202. https://doi.org/10.1097/pas.0000000000000662
16. Dasari A, Shen C, Halperin D, et al. (2017) Trends in the incidence, prevalence, and survival outcomes in patients with neuroendocrine tumors in the united states. JAMA Oncol 3 (10):1335-1342. https://doi.org/10.1001/jamaoncol.2017.0589
17. Sho S, Court CM, Winograd P, Toste PA, Pisegna JR, Lewis M, Donahue TR, Hines OJ, Reber HA, Dawson DW, Tomlinson JS (2018) A Prognostic Scoring System for the Prediction of Metastatic Recurrence Following Curative Resection of Pancreatic Neuroendocrine Tumors. J Gastrointest Surg. https://doi.org/10.1007/s11605-018-4011-7
18. Jensen RT, Cadiot G, Brandi ML, de Herder WW, Kaltsas G, Komminoth P, Scoazec J-Y, Salazar R, Sauvanet A, Kianmanesh R (2012) ENETS Consensus Guidelines for the Management of Patients with Digestive Neuroendocrine Neoplasms: Functional Pancreatic Endocrine Tumor Syndromes. Neuroendocrinology 95 (2):98-119. https://doi.org/10.1159/000335591
19. Sadowski SM, Neychev V, Millo C, Shih J, Nilubol N, Herscovitch P, Pacak K, Marx SJ, Kebebew E (2016) Prospective Study of 68Ga-DOTATATE Positron Emission Tomography/Computed Tomography for Detecting Gastro-Entero-Pancreatic Neuroendocrine Tumors and Unknown Primary Sites. J Clin Oncol 34 (6):588-596. https://doi.org/10.1200/jco.2015.64.0987
20. Buchmann I, Henze M, Engelbrecht S, Eisenhut M, Runz A, Schafer M, Schilling T, Haufe S, Herrmann T, Haberkorn U (2007) Comparison of 68Ga-DOTATOC PET and 111In-DTPAOC (Octreoscan) SPECT in patients with neuroendocrine tumours. Eur J Nucl Med Mol Imaging 34 (10):1617-1626. https://doi.org/10.1007/s00259-007-0450-1
21. Oberndorfer S (1907) Karzinoide tumoren des dunndarms. Frankfurt Z Path 1:426-432
22. Öberg KE (2010) Gastrointestinal neuroendocrine tumors. Annals of Oncology 21 (suppl_7):vii72-vii80
23. Triponez F, Dosseh D, Goudet P, Cougard P, Bauters C, Murat A, Cadiot G, Niccoli-Sire P, Chayvialle JA, Calender A, Proye CA (2006) Epidemiology data on 108 MEN 1 patients from the GTE with isolated nonfunctioning tumors of the pancreas. Ann Surg 243 (2):265-272. https://doi.org/10.1097/01.sla.0000197715.96762.68
24. Corrias G, Monti S, Horvat N, Tang L, Basturk O, Saba L, Mannelli L (2018) Imaging features of malignant abdominal neuroendocrine tumors with rare presentation. Clin Imaging 51:59-64. https://doi.org/10.1016/j.clinimag.2018.02.004
25. Owen N, Sohaib S, Peppercorn P, Monson J, Grossman A, Besser G, Reznek R (2001) MRI of pancreatic neuroendocrine tumours. The British journal of radiology 74 (886):968-973
26. Kim JH, Eun HW, Kim YJ, Han JK, Choi BI (2013) Staging accuracy of MR for pancreatic neuroendocrine tumor and imaging findings according to the tumor grade. Abdominal imaging 38 (5):1106-1114
27. Metz DC, Jensen RT (2008) Gastrointestinal neuroendocrine tumors: pancreatic endocrine tumors. Gastroenterology 135 (5):1469-1492
28. Guo J, Zhao J, Bi X, Li Z, Huang Z, Zhang Y, Cai J, Zhao H (2017) Should surgery be conducted for small nonfunctioning pancreatic neuroendocrine tumors: a systematic review. Oncotarget 8 (21):35368-35375. https://doi.org/10.18632/oncotarget.15685
29. Raman SP, Hruban RH, Cameron JL, Wolfgang CL, Fishman EK (2012) Pancreatic imaging mimics: part 2, pancreatic neuroendocrine tumors and their mimics. AJR Am J Roentgenol 199 (2):309-318. https://doi.org/10.2214/ajr.12.8627
30. Foster DS, Jensen R, Norton JA (2018) Management of liver neuroendocrine tumors in 2018. JAMA Oncol. https://doi.org/10.1001/jamaoncol.2018.3035
31. Ito T, Igarashi H, Uehara H, Berna MJ, Jensen RT (2013) Causes of death and prognostic factors in multiple endocrine neoplasia type 1: a prospective study: comparison of 106 MEN1/Zollinger-Ellison syndrome patients with 1613 literature MEN1 patients with or without pancreatic endocrine tumors. Medicine (Baltimore) 92 (3):135-181. https://doi.org/10.1097/md.0b013e3182954af1
32. Reznek RH (2006) CT/MRI of neuroendocrine tumours. Cancer Imaging 6 (Spec No A):S163-S177. https://doi.org/10.1102/1470-7330.2006.9037
33. Lipinski M, Rydzewska G, Foltyn W, Andrysiak-Mamos E, Baldys-Waligorska A, Bednarczuk T, Blicharz-Dorniak J, Bolanowski M, Boratyn-Nowicka A, Borowska M, Cichocki A, Cwikla JB, Falconi M, Handkiewicz-Junak D, Hubalewska-Dydejczyk A, Jarzab B, Junik R, Kajdaniuk D, Kaminski G, Kolasinska-Cwikla A, Kowalska A, Krol R, Krolicki L, Kunikowska J, Kusnierz K, Lampe P, Lange D, Lewczuk-Myslicka A, Lewinski A, Londzin-Olesik M, Marek B, Nasierowska-Guttmejer A, Nowakowska-Dulawa E, Pilch-Kowalczyk J, Poczkaj K, Rosiek V, Ruchala M, Sieminska L, Sowa-Staszczak A, Starzynska T, Steinhof-Radwanska K, Strzelczyk J, Sworczak K, Syrenicz A, Szawlowski A, Szczepkowski M, Wachula E, Zajecki W, Zemczak A, Zgliczynski W, Kos-Kudla B (2017) Gastroduodenal neuroendocrine neoplasms, including gastrinoma - management guidelines (recommended by the Polish Network of Neuroendocrine Tumours). Endokrynol Pol 68 (2):138-153. https://doi.org/10.5603/ep.2017.0016

34. O'Toole D, Salazar R, Falconi M, Kaltsas G, Couvelard A, de Herder WW, Hyrdel R, Nikou G, Krenning E, Vullierme M-P (2006) Rare functioning pancreatic endocrine tumors. Neuroendocrinology 84 (3):189-195
35. Lo GC, Kambadakone A (2018) MR Imaging of Pancreatic Neuroendocrine Tumors. Magn Reson Imaging Clin N Am 26 (3):391-403. https://doi.org/10.1016/j.mric.2018.03.010
36. Lee NJ, Hruban RH, Fishman EK (2018) Pancreatic neuroendocrine tumor: review of heterogeneous spectrum of CT appearance. Abdom Radiol (NY) 43 (11):3025-3034. https://doi.org/10.1007/s00261-018-1574-4
37. Bushnell DL, Baum RP (2011) Standard imaging techniques for neuroendocrine tumors. Endocrinol Metab Clin North Am 40 (1):153-162, ix. https://doi.org/10.1016/j.ecl.2010.12.002
38. Sundin A, Garske U, Örlefors H Nuclear imaging of neuroendocrine tumours. Best Practice & Research Clinical Endocrinology & Metabolism 21 (1):69-85. https://doi.org/10.1016/j.beem.2006.12.003
39. Sun H, Zhou J, Liu K, Shen T, Wang X, Wang X (2018) Pancreatic neuroendocrine tumors: MR imaging features preoperatively predict lymph node metastasis. Abdom Radiol (NY). https://doi.org/10.1007/s00261-018-1863-y
40. Dromain C, Deandreis D, Scoazec JY, Goere D, Ducreux M, Baudin E, Tselikas L (2016) Imaging of neuroendocrine tumors of the pancreas. Diagn Interv Imaging 97 (12):1241-1257. https://doi.org/10.1016/j.diii.2016.07.012
41. Boninsegna L, Partelli S, D'Innocenzio MM, Capelli P, Scarpa A, Bassi C, Pederzoli P, Falconi M (2010) Pancreatic cystic endocrine tumors: a different morphological entity associated with a less aggressive behavior. Neuroendocrinology 92 (4):246-251. https://doi.org/10.1159/000318771
42. Singhi AD, Chu LC, Tatsas AD, Shi C, Ellison TA, Fishman EK, Kawamoto S, Schulick RD, Wolfgang CL, Hruban RH, Edil BH (2012) Cystic Pancreatic Neuroendocrine Tumors: A Clinicopathologic Study. The American Journal of Surgical Pathology 36 (11):1666-1673. https://doi.org/10.1097/pas.0b013e31826a0048
43. De Robertis R, Maris B, Cardobi N, Tinazzi Martini P, Gobbo S, Capelli P, Ortolani S, Cingarlini S, Paiella S, Landoni L, Butturini G, Regi P, Scarpa A, Tortora G, D'Onofrio M (2018) Can histogram analysis of MR images predict aggressiveness in pancreatic neuroendocrine tumors? Eur Radiol. https://doi.org/10.1007/s00330-017-5236-7
44. Buetow PC, Buck JL, Pantongrag-Brown L, Beck KG, Ros PR, Adair CF (1996) Solid and papillary epithelial neoplasm of the pancreas: imaging-pathologic correlation on 56 cases. Radiology 199 (3):707-711
45. Semelka RC, Ascher SM (1993) MR imaging of the pancreas. Radiology 188 (3):593-602
46. Sureka B, Meena V, Khera PS (2018) Differential diagnosis of pancreatic calcifications. American Journal of Roentgenology 210 (1):W43-W43
47. Javadi S, Menias CO, Korivi BR, Shaaban AM, Patnana M, Alhalabi K, Elsayes KM (2017) Pancreatic calcifications and calcified pancreatic masses: pattern recognition approach on CT. American Journal of Roentgenology 209 (1):77-87
48. Singh R, Calhoun S, Shin M, Katz R (2008) Pancreatic Neuroendocrine Tumor with Atypical Radiologic Presentation. Radiol Case Rep 3 (3):162. https://doi.org/10.2484/rcr.v3i3.162
49. Cescato R, Schulz S, Waser B, Eltschinger V, Rivier JE, Wester HJ, Culler M, Ginj M, Liu Q, Schonbrunn A, Reubi JC (2006) Internalization of sst2, sst3, and sst5 receptors: effects of somatostatin agonists and antagonists. J Nucl Med 47 (3):502-511
50. Graham MM, Gu X, Ginader T, Breheny P, Sunderland JJ (2017) (68)Ga-DOTATOC Imaging of Neuroendocrine Tumors: A Systematic Review and Metaanalysis. J Nucl Med 58 (9):1452-1458. https://doi.org/10.2967/jnumed.117.191197
51. Reubi JC, Waser B, Friess H, Büchler M, Laissue J (1998) Neurotensin receptors: a new marker for human ductal pancreatic adenocarcinoma. Gut 42 (4):546
52. Stabin MG, Kooij PP, Bakker WH, Inoue T, Endo K, Coveney J, de Jong R, Minegishi A (1997) Radiation dosimetry for indium-111-pentetreotide. J Nucl Med 38 (12):1919-1922
53. Sandstrom M, Velikyan I, Garske-Roman U, Sorensen J, Eriksson B, Granberg D, Lundqvist H, Sundin A, Lubberink M (2013) Comparative biodistribution and radiation dosimetry of 68Ga-DOTATOC and 68Ga-DOTATATE in patients with neuroendocrine tumors. J Nucl Med 54 (10):1755-1759. https://doi.org/10.2967/jnumed.113.120600
54. Werner RA, Bluemel C, Allen-Auerbach MS, Higuchi T, Herrmann K (2015) 68 Gallium-and 90 Yttrium-/177 Lutetium:"theranostic twins" for diagnosis and treatment of NETs. Annals of nuclear medicine 29 (1):1-7
55. Kabasakal L, Demirci E, Ocak M, Decristoforo C, Araman A, Ozsoy Y, Uslu I, Kanmaz B (2012) Comparison of (6)(8)Ga-DOTATATE and (6)(8)Ga-DOTANOC PET/CT imaging in the same patient group with neuroendocrine tumours. Eur J Nucl Med Mol Imaging 39 (8):1271-1277. https://doi.org/10.1007/s00259-012-2123-y
56. Fani M, Nicolas GP, Wild D (2017) Somatostatin receptor antagonists for imaging and therapy. J Nucl Med 58 (Suppl 2):61S-66S
57. Kauhanen S, Seppanen M, Nuutila P (2008) Premedication with carbidopa masks positive finding of insulinoma and beta-cell hyperplasia in [(18)F]-dihydroxy-phenyl-alanine positron emission tomography. J Clin Oncol 26 (32):5307-5308; author reply 5308-5309. https://doi.org/10.1200/jco.2008.18.8581
58. Halbrook CJ, Lyssiotis CA (2017) Employing Metabolism to Improve the Diagnosis and Treatment of Pancreatic Cancer. Cancer Cell 31 (1):5-19. https://doi.org/10.1016/j.ccell.2016.12.006
59. Vander Heiden MG, Cantley LC, Thompson CB (2009) Understanding the Warburg effect: the metabolic requirements of cell proliferation. Science 324 (5930):1029-1033. https://doi.org/10.1126/science.1160809
60. Binderup T, Knigge U, Loft A, Federspiel B, Kjaer A (2010) 18F-fluorodeoxyglucose positron emission tomography predicts survival of patients with neuroendocrine tumors. Clin Cancer Res 16 (3):978-985. https://doi.org/10.1158/1078-0432.ccr-09-1759
61. Hindie E (2017) The NETPET Score: Combining FDG and Somatostatin Receptor Imaging for Optimal Management of Patients with Metastatic Well-Differentiated Neuroendocrine Tumors. Theranostics 7 (5):1159-1163. https://doi.org/10.7150/thno.19588
62. Bucau M, Laurent-Bellue A, Poté N, Hentic O, Cros J, Mikail N, Rebours V, Ruszniewski P, Lebtahi R, Couvelard A (2018) 18F-FDG Uptake in Well-Differentiated Neuroendocrine Tumors Correlates with Both Ki-67 and VHL Pathway Inactivation. Neuroendocrinology 106 (3):274-282
63. Zimny M, Bares R, Fass J, Adam G, Cremerius U, Dohmen B, Klever P, Sabri O, Schumpelick V, Buell U (1997) Fluorine-18 fluorodeoxyglucose positron emission tomography in the differential diagnosis of pancreatic carcinoma: a report of 106 cases. European journal of nuclear medicine 24 (6):678-682
64. Korner M, Stockli M, Waser B, Reubi JC (2007) GLP-1 receptor expression in human tumors and human normal tissues: potential for in vivo targeting. J Nucl Med 48 (5):736-743. https://doi.org/10.2967/jnumed.106.038679
65. Sowa-Staszczak A, Pach D, Mikolajczak R, Macke H, Jabrocka-Hybel A, Stefanska A, Tomaszuk M, Janota B, Gilis-Januszewska A, Malecki M, Kaminski G, Kowalska A, Kulig J, Matyja A, Osuch C, Hubalewska-Dydejczyk A (2013) Glucagon-like peptide-1 receptor imaging with [Lys40(Ahx-HYNIC- 99mTc/EDDA)NH2]-exendin-4 for the detection of

insulinoma. Eur J Nucl Med Mol Imaging 40 (4):524-531. https://doi.org/10.1007/s00259-012-2299-1
66. Sowa-Staszczak A, Trofimiuk-Müldner M, Stefańska A, Tomaszuk M, Buziak-Bereza M, Gilis-Januszewska A, Jabrocka-Hybel A, Głowa B, Małecki M, Bednarczuk T (2016) 99mTc labeled glucagon-like peptide-1-analogue (99mTc-GLP1) scintigraphy in the management of patients with occult insulinoma. PloS one 11 (8):e0160714
67. Christ E, Wild D, Ederer S, Béhé M, Nicolas G, Caplin ME, Brändle M, Clerici T, Fischli S, Stettler C (2013) Glucagon-like peptide-1 receptor imaging for the localisation of insulinomas: a prospective multicentre imaging study. The Lancet Diabetes & Endocrinology 1 (2):115-122
68. Doppman JL, Miller DL, Chang R, Shawker TH, Gorden P, Norton JA (1991) Insulinomas: localization with selective intraarterial injection of calcium. Radiology 178 (1):237-241
69. Braatvedt G, Jennison E, Holdaway IM (2014) Comparison of two low-dose calcium infusion schedules for localization of insulinomas by selective pancreatic arterial injection with hepatic venous sampling for insulin. Clinical endocrinology 80 (1):80-84
70. Kato M, Doi R, Imamura M, Furutani M, Hosotani R, Shimada Y (1997) Calcium-evoked insulin release from insulinoma cells is mediated via calcium-sensing receptor. Surgery 122 (6):1203-1211
71. Itami A, Kato M, Komoto I, Doi R, Hosotani R, Shimada Y, Imamura M (2001) Human gastrinoma cells express calcium-sensing receptor. Life Sciences 70 (2):119-129. https://doi.org/10.1016/s0024-3205(01)01380-7
72. Morganstein D, Lewis D, Jackson J, Isla A, Lynn J, Devendra D, Meeran K, Todd J (2009) The role of arterial stimulation and simultaneous venous sampling in addition to cross-sectional imaging for localisation of biochemically proven insulinoma. Eur Radiol 19 (10):2467-2473
73. Yeh R, Dercle L, Garg I, Wang ZJ, Hough DM, Goenka AH (2018) The Role of 18F-FDG PET/CT and PET/MRI in Pancreatic Ductal Adenocarcinoma. Abdominal Radiology 43 (2):415-434
74. Attenberger U, Catana C, Chandarana H, Catalano OA, Friedman K, Schonberg SA, Thrall J, Salvatore M, Rosen BR, Guimaraes AR (2015) Whole-body FDG PET-MR oncologic imaging: pitfalls in clinical interpretation related to inaccurate MR-based attenuation correction. Abdominal Imaging 40 (6):1374-1386. https://doi.org/10.1007/s00261-015-0455-3
75. Kamisawa T, Takum K, Anjiki H, Egawa N, Kurata M, Honda G, Tsuruta K (2010) FDG-PET/CT findings of autoimmune pancreatitis. Hepato-gastroenterology 57 (99-100):447-450
76. Kato K, Nihashi T, Ikeda M, Abe S, Iwano S, Itoh S, Shimamoto K, Naganawa S (2013) Limited Efficacy of 18F-FDG PET/CT for Differentiation Between Metastasis-Free Pancreatic Cancer and Mass-Forming Pancreatitis. Clinical Nuclear Medicine 38 (6):417. https://doi.org/10.1097/rlu.0b013e3182817d9d
77. Matsumoto I, Shirakawa S, Shinzeki M, Asari S, Goto T, Ajiki T, Fukumoto T, Kitajima K, Ku Y (2013) 18-Fluorodeoxyglucose Positron Emission Tomography Does Not Aid in Diagnosis of Pancreatic Ductal Adenocarcinoma. Clinical Gastroenterology and Hepatology 11 (6):712-718. https://doi.org/10.1016/j.cgh.2012.12.033
78. Rijkers AP, Valkema R, Duivenvoorden HJ, van Eijck CHJ (2014) Usefulness of F-18-fluorodeoxyglucose positron emission tomography to confirm suspected pancreatic cancer: A meta-analysis. European Journal of Surgical Oncology (EJSO) 40 (7):794-804. https://doi.org/10.1016/j.ejso.2014.03.016
79. Beiderwellen K, Geraldo L, Ruhlmann V, Heusch P, Gomez B, Nensa F, Umutlu L, Lauenstein TC (2015) Accuracy of [18F] FDG PET/MRI for the Detection of Liver Metastases. PLoS One 10 (9):e0137285. https://doi.org/10.1371/journal.pone.0137285
80. Joo I, Lee JM, Lee DH, Lee ES, Paeng JC, Lee SJ, Jang JY, Kim SW, Ryu JK, Lee KB (2017) Preoperative Assessment of Pancreatic Cancer with FDG PET/MR Imaging versus FDG PET/CT Plus Contrast-enhanced Multidetector CT: A Prospective Preliminary Study. Radiology 282 (1):149-159. https://doi.org/10.1148/radiol.2016152798
81. Schaarschmidt BM, Grueneisen J, Heusch P, Gomez B, Umutlu L, Ruhlmann V, Rosenbaum-Krumme S, Antoch G, Buchbender C (2015) Does 18F-FDG PET/MRI reduce the number of indeterminate abdominal incidentalomas compared with 18F-FDG PET/CT? Nucl Med Commun 36 (6):588-595. https://doi.org/10.1097/mnm.0000000000000298
82. Chen BB, Tien YW, Chang MC, Cheng MF, Chang YT, Yang SH, Wu CH, Kuo TC, Shih IL, Yen RF, Shih TT (2018) Multiparametric PET/MR imaging biomarkers are associated with overall survival in patients with pancreatic cancer. Eur J Nucl Med Mol Imaging 45 (7):1205-1217. https://doi.org/10.1007/s00259-018-3960-0
83. Dercle L, Deandreis D, Terroir M, Leboulleux S, Lumbroso J, Schlumberger M (2016) Evaluation of 124 I PET/CT and 124 I PET/MRI in the management of patients with differentiated thyroid cancer. European journal of nuclear medicine and molecular imaging 43 (6):1006-1010
84. Kolbitsch C, Neji R, Fenchel M, Mallia A, Marsden P, Schaeffter T (2018) Fully integrated 3D high-resolution multicontrast abdominal PET-MR with high scan efficiency. Magn Reson Med 79 (2):900-911. https://doi.org/10.1002/mrm.26757
85. Fuin N, Catalano OA, Scipioni M, Canjels LPW, Izquierdo-Garcia D, Pedemonte S, Catana C (2018) Concurrent Respiratory Motion Correction of Abdominal PET and Dynamic Contrast-Enhanced-MRI Using a Compressed Sensing Approach. J Nucl Med 59 (9):1474-1479. https://doi.org/10.2967/jnumed.117.203943
86. Yang J, Liu J, Wiesinger F, Menini A, Zhu X, Hope TA, Seo Y, Larson PEZ (2018) Developing an efficient phase-matched attenuation correction method for quiescent period PET in abdominal PET/MRI. Phys Med Biol 63 (18):185002. https://doi.org/10.1088/1361-6560/aada26
87. Wagenknecht G, Kaiser HJ, Mottaghy FM, Herzog H (2013) MRI for attenuation correction in PET: methods and challenges. MAGMA 26 (1):99-113. https://doi.org/10.1007/s10334-012-0353-4
88. Keereman V, Mollet P, Berker Y, Schulz V, Vandenberghe S (2013) Challenges and current methods for attenuation correction in PET/MR. MAGMA 26 (1):81-98. https://doi.org/10.1007/s10334-012-0334-7
89. Visvikis D, Monnier F, Bert J, Hatt M, Fayad H (2014) PET/MR attenuation correction: where have we come from and where are we going? Eur J Nucl Med Mol Imaging 41 (6):1172-1175. https://doi.org/10.1007/s00259-014-2748-0
90. Attenberger U, Catana C, Chandarana H, Catalano OA, Friedman K, Schonberg SA, Thrall J, Salvatore M, Rosen BR, Guimaraes AR (2015) Whole-body FDG PET-MR oncologic imaging: pitfalls in clinical interpretation related to inaccurate MR-based attenuation correction. Abdom Imaging 40 (6):1374-1386. https://doi.org/10.1007/s00261-015-0455-3
91. Martinez-Moller A, Souvatzoglou M, Delso G, Bundschuh RA, Chefd'hotel C, Ziegler SI, Navab N, Schwaiger M, Nekolla SG (2009) Tissue classification as a potential approach for attenuation correction in whole-body PET/MRI: evaluation with PET/CT data. J Nucl Med 50 (4):520-526. https://doi.org/10.2967/jnumed.108.054726
92. Jeong JH, Cho IH, Kong EJ, Chun KA (2014) Evaluation of Dixon Sequence on Hybrid PET/MR Compared with Contrast-Enhanced PET/CT for PET-Positive Lesions. Nucl Med Mol Imaging 48 (1):26-32. https://doi.org/10.1007/s13139-013-0240-6

93. Dercle L, Lu L, Lichtenstein P, Yang H, Wang D, Zhu J, Wu F, Piessevaux H, Schwartz LH, Zhao B (2017) Impact of Variability in Portal Venous Phase Acquisition Timing in Tumor Density Measurement and Treatment Response Assessment: Metastatic Colorectal Cancer as a Paradigm. JCO Clinical Cancer Informatics (1):1-8. https://doi.org/10.1200/cci.17.00108
94. Dercle L, Chisin R, Ammari S, Gillebert Q, Ouali M, Jaudet C, Delord JP, Dierickx L, Zerdoud S, Schlumberger M, Courbon F (2014) Nonsurgical giant cell tumour of the tendon sheath or of the diffuse type: Are MRI or F-FDG PET/CT able to provide an accurate prediction of long-term outcome? Eur J Nucl Med Mol Imaging. https://doi.org/10.1007/s00259-014-2938-9
95. Dercle L, Ammari S, Bateson M, Durand PB, Haspinger E, Massard C, Jaudet C, Varga A, Deutsch E, Soria JC, Ferte C (2017) Limits of radiomic-based entropy as a surrogate of tumor heterogeneity: ROI-area, acquisition protocol and tissue site exert substantial influence. Sci Rep 7 (1):7952. https://doi.org/10.1038/s41598-017-08310-5
96. Dierickx LO, Dercle L, Chaltiel L, Caselles O, Brillouet S, Zerdoud S, Courbon F (2017) Evaluation of 2 diuretic 18Fluorine-Fluorodeoxyglucose positron emission tomography/computed tomography imaging protocols for intra-pelvic cancer. Q J Nucl Med Mol Imaging. https://doi.org/10.23736/s1824-4785.17.02912-0
97. Sun R, Limkin EJ, Dercle L, Reuze S, Zacharaki EI, Chargari C, Schernberg A, Dirand AS, Alexis A, Paragios N, Deutsch E, Ferte C, Robert C (2017) [Computational medical imaging (radiomics) and potential for immuno-oncology]. Cancer Radiother 21 (6-7):648-654. https://doi.org/10.1016/j.canrad.2017.07.035
98. Dercle L, Hartl D, Rozenblum-Beddok L, Mokrane FZ, Seban RD, Yeh R, Bidault F, Ammari S (2018) Diagnostic and prognostic value of 18F-FDG PET, CT, and MRI in perineural spread of head and neck malignancies. Eur Radiol 28 (4):1761-1770. https://doi.org/10.1007/s00330-017-5063-x
99. Chi W, Warner RRP, Chan DL, Singh S, Segelov E, Strosberg J, Wisnivesky J, Kim MK (2018) Long-term Outcomes of Gastroenteropancreatic Neuroendocrine Tumors. Pancreas 47 (3):321. https://doi.org/10.1097/mpa.0000000000001005
100. Patel BN, Olcott E, Jeffrey RB (2018) Extrapancreatic perineural invasion in pancreatic adenocarcinoma. Abdom Radiol (NY) 43 (2):323-331. https://doi.org/10.1007/s00261-017-1343-9
101. De Robertis R, Paiella S, Cardobi N, Landoni L, Tinazzi Martini P, Ortolani S, De Marchi G, Gobbo S, Giardino A, Butturini G, Tortora G, Bassi C, D'Onofrio M (2018) Tumor thrombosis: a peculiar finding associated with pancreatic neuroendocrine neoplasms. A pictorial essay. Abdom Radiol (NY) 43 (3):613-619. https://doi.org/10.1007/s00261-017-1243-z
102. Kulke MH, Anthony LB, Bushnell DL, De Herder WW, Goldsmith SJ, Klimstra DS, Marx SJ, Pasieka JL, Pommier RF, Yao JC (2010) NANETS treatment guidelines: well-differentiated neuroendocrine tumors of the stomach and pancreas. Pancreas 39 (6):735
103. Sundin A, Arnold R, Baudin E, Cwikla JB, Eriksson B, Fanti S, Fazio N, Giammarile F, Hicks RJ, Kjaer A, Krenning E, Kwekkeboom D, Lombard-Bohas C, O'Connor JM, O'Toole D, Rockall A, Wiedenmann B, Valle JW, Vullierme M-P, all other Antibes Consensus Conference p (2017) ENETS Consensus Guidelines for the Standards of Care in Neuroendocrine Tumors: Radiological, Nuclear Medicine and Hybrid Imaging. Neuroendocrinology 105 (3):212-244. https://doi.org/10.1159/000471879
104. Schraml C, Schwenzer NF, Sperling O, Aschoff P, Lichy MP, Muller M, Brendle C, Werner MK, Claussen CD, Pfannenberg C (2013) Staging of neuroendocrine tumours: comparison of [(6)(8)Ga]DOTATOC multiphase PET/CT and whole-body MRI. Cancer Imaging 13:63-72. https://doi.org/10.1102/1470-7330.2013.0007
105. Yu F, Venzon DJ, Serrano J, Goebel SU, Doppman JL, Gibril F, Jensen RT (1999) Prospective study of the clinical course, prognostic factors, causes of death, and survival in patients with long-standing Zollinger-Ellison syndrome. J Clin Oncol 17 (2):615-630. https://doi.org/10.1200/jco.1999.17.2.615
106. Jensen RT, Niederle B, Mitry E, Ramage JK, Steinmuller T, Lewington V, Scarpa A, Sundin A, Perren A, Gross D, O'Connor JM, Pauwels S, Kloppel G, Frascati Consensus C, European Neuroendocrine Tumor S (2006) Gastrinoma (duodenal and pancreatic). Neuroendocrinology 84 (3):173-182. https://doi.org/10.1159/000098009
107. Ellison EC, Johnson JA (2009) The Zollinger-Ellison syndrome: a comprehensive review of historical, scientific, and clinical considerations. Current problems in surgery 46 (1):13-106
108. d'Assignies G, Fina P, Bruno O, Vullierme MP, Tubach F, Paradis V, Sauvanet A, Ruszniewski P, Vilgrain V (2013) High sensitivity of diffusion-weighted MR imaging for the detection of liver metastases from neuroendocrine tumors: comparison with T2-weighted and dynamic gadolinium-enhanced MR imaging. Radiology 268 (2):390-399. https://doi.org/10.1148/radiol.13121628
109. Pavel M, Baudin E, Couvelard A, Krenning E, Oberg K, Steinmuller T, Anlauf M, Wiedenmann B, Salazar R, Barcelona Consensus Conference p (2012) ENETS Consensus Guidelines for the management of patients with liver and other distant metastases from neuroendocrine neoplasms of foregut, midgut, hindgut, and unknown primary. Neuroendocrinology 95 (2):157-176. https://doi.org/10.1159/000335597
110. Hope TA, Bergsland EK, Bozkurt MF, Graham M, Heaney AP, Herrmann K, Howe JR, Kulke MH, Kunz PL, Mailman J, May L, Metz DC, Millo C, O'Dorisio S, Reidy-Lagunes DL, Soulen MC, Strosberg JR (2018) Appropriate Use Criteria for Somatostatin Receptor PET Imaging in Neuroendocrine Tumors. J Nucl Med 59 (1):66-74. https://doi.org/10.2967/jnumed.117.202275
111. Orditura M, Petrillo A, Ventriglia J, Diana A, Laterza MM, Fabozzi A, Savastano B, Franzese E, Conzo G, Santini L, Ciardiello F, De Vita F (2016) Pancreatic neuroendocrine tumors: Nosography, management and treatment. Int J Surg 28 Suppl 1:S156-162. https://doi.org/10.1016/j.ijsu.2015.12.052
112. Dromain C, de Baere T, Lumbroso J, Caillet H, Laplanche A, Boige V, Ducreux M, Duvillard P, Elias D, Schlumberger M, Sigal R, Baudin E (2005) Detection of liver metastases from endocrine tumors: a prospective comparison of somatostatin receptor scintigraphy, computed tomography, and magnetic resonance imaging. J Clin Oncol 23 (1):70-78. https://doi.org/10.1200/jco.2005.01.013
113. de Baère T, Aupérin A, Deschamps F, Chevallier P, Gaubert Y, Boige V, Fonck M, Escudier B, Palussiére J (2015) Radiofrequency ablation is a valid treatment option for lung metastases: experience in 566 patients with 1037 metastases. Annals of Oncology 26 (5):987-991. https://doi.org/10.1093/annonc/mdv037
114. Eriksson J, Stålberg P, Nilsson A, Krause J, Lundberg C, Skogseid B, Granberg D, Eriksson B, Åkerström G, Hellman P (2008) Surgery and Radiofrequency Ablation for Treatment of Liver Metastases from Midgut and Foregut Carcinoids and Endocrine Pancreatic Tumors. World J Surg 32 (5):930-938. https://doi.org/10.1007/s00268-008-9510-3
115. de Baere T, Palussiere J, Auperin A, Hakime A, Abdel-Rehim M, Kind M, Dromain C, Ravaud A, Tebboune N, Boige V, Malka D, Lafont C, Ducreux M (2006) Midterm local efficacy and survival after radiofrequency ablation of lung tumors with minimum follow-up of 1 year: prospective evaluation. Radiology 240 (2):587-596. https://doi.org/10.1148/radiol.2402050807
116. Kennedy A, Bester L, Salem R, Sharma RA, Parks RW, Ruszniewski P (2015) Role of hepatic intra-arterial therapies in

metastatic neuroendocrine tumours (NET): guidelines from the NET-Liver-Metastases Consensus Conference. HPB (Oxford) 17 (1):29-37. https://doi.org/10.1111/hpb.12326

117. Vogl TJ, Gruber T, Naguib NNN, Hammerstingl R, Nour-Eldin N-EA (2009) Liver metastases of neuroendocrine tumors: treatment with hepatic transarterial chemotherapy using two therapeutic protocols. American Journal of Roentgenology 193 (4):941-947